An Invitation to LaTeX

Xiang Gao, Lecturer

E-mail: xgao@ouc.edu.cn | Web: https://ouc-xgao.github.io/

College of Engineering, Ocean University of China

课程大纲

- LaTeX一览
- LaTeX基础
- LaTeX公式
- LaTeX进阶

课程大纲

- LaTeX一览
  - LaTeX简介
  - 课程简介
  - 模板示例
- LaTeX基础
- LaTeX公式
- LaTeX进阶

LaTeX简介

- 什么是LaTeX, What?
  - LaTeX是一种用于进行高质量排版的文档处理系统
  - LaTeX被广泛的用于排版大中型科学技术文献
  - LaTeX几乎能用于排版任何形式的出版物

LaTeX简介

- 什么是LaTeX, What?
  - LaTeX是一种用于进行高质量排版的文档处理系统
  - LaTeX被广泛的用于排版大中型科学技术文献
  - LaTeX几乎能用于排版任何形式的出版物
- 为什么要用LaTeX, Why?
  - LaTeX是免费、多平台的
  - LaTeX只是一种文本文件，并且能很容易的转换成 PDF
  - LaTeX的内容和格式是分离的，一旦设定好风格，就能专注于内容
  - LaTeX比MSWord工作流程更快
  - LaTeX被广泛的用于科学主题中
  - LaTeX是排版数学公式的最佳选择

LaTeX简介

- 怎样用好LaTeX, How?
  - **R**ead：阅读采用LaTeX生成的论文
  - **S**earch：查找不熟悉的LaTeX命令
  - **T**rain：练习采用LaTeX进行文章排版

LaTeX简介

- 怎样用好LaTeX, How?
  - **R**ead：阅读采用LaTeX生成的论文
  - **S**earch：查找不熟悉的LaTeX命令
  - **T**rain：练习采用LaTeX进行文章排版
- LaTeX（可以忽略）的不足之处
  - 入门门槛较高
  - 不易排查错误
  - 不易定制样式
  - 非所见即所得
  - 表格排版繁琐

LaTeX简介

- 怎样用好LaTeX, How?
  - Read：阅读采用LaTeX生成的论文
  - Search：查找不熟悉的LaTeX命令
  - Train：练习采用LaTeX进行文章排版
- LaTeX（可以忽略）的不足之处
  - 入门门槛较高
  - 不易排查错误
  - 不易定制样式
  - 非所见即所得
  - 表格排版繁琐

TABLE III
COMPARISON EXPERIMENT RESULTS ON THE EVALUATION DATASETS.

Data	Weiszfeld [8]	ℓ_1-IRLS [10]	ℓ_1-IRLS($\ell_{\frac{1}{2}}$) [11]	OMSTs [17]	Proposed method
ELS	1.66	1.02	1.15	0.75	0.59
PDP	3.35	2.19	2.62	1.73	0.92
NYC	2.43	1.43	1.40	1.30	1.24
MDR	4.37	2.75	3.08	1.12	2.54
YKM	2.73	1.71	1.62	1.55	1.57
MND	0.92	0.77	0.71	0.68	0.62
TOL	2.73	2.55	2.45	2.10	2.05
ALM	3.57	2.12	2.14	1.26	1.03
GDM	—	39.15	28.20	45.15	4.04
VNC	5.14	4.47	4.64	3.30	1.84
USQ	13.54	4.34	4.97	3.83	3.77
ROF	2.11	1.59	1.70	1.85	2.48
PIC	7.65	2.38	3.12	1.41	4.87
TFG	13.20	1.85	2.03	2.63	4.88
SNF	15.85	3.05	3.56	3.26	2.85

```
\begin{table}
\centering
\scriptsize
\caption{{Comparison experiment results on the evaluation datasets.}}
\begin{tabular}{l|cccc|c}\Xhline{1pt}
\multirow{2}*{Data} & Weiszfeld & $\ell_1$-IRLS & $\ell_1$-IRLS($\ell_{\frac{1}{2}}$) & OMSTs & Proposed\\
& \cite{Hartley-CVPR-11} & \cite{Chatterjee-ICCV-13} & \cite{Chatterjee-TPAMI-18} & \cite{Cui-ISPRS-19} & method\\\Xhline{0.5pt}
ELS & $1.66$ & \cellcolor{color_3rd}{$1.02$} & \cellcolor{color_4th}{$1.15$} & \cellcolor{color_2nd}{$0.75$} & \cellcolor{color_1st}{$0.59$}\\
PDP & $3.35$ & \cellcolor{color_3rd}{$2.19$} & \cellcolor{color_4th}{$2.62$} & \cellcolor{color_2nd}{$1.73$} & \cellcolor{color_1st}{$0.92$}\\
NYC & $2.43$ & \cellcolor{color_4th}{$1.43$} & \cellcolor{color_3rd}{$1.40$} & \cellcolor{color_2nd}{$1.30$} & \cellcolor{color_1st}{$1.24$}\\
MDR & $4.37$ & \cellcolor{color_3rd}{$2.75$} & \cellcolor{color_4th}{$3.08$} & \cellcolor{color_1st}{$1.12$} & \cellcolor{color_2nd}{$2.54$}\\
YKM & $2.73$ & \cellcolor{color_4th}{$1.71$} & \cellcolor{color_3rd}{$1.62$} & \cellcolor{color_1st}{$1.55$} & \cellcolor{color_2nd}{$1.57$}\\
MND & $0.92$ & \cellcolor{color_4th}{$0.77$} & \cellcolor{color_3rd}{$0.71$} & \cellcolor{color_2nd}{$0.68$} & \cellcolor{color_1st}{$0.62$}\\
TOL & $2.73$ & \cellcolor{color_4th}{$2.55$} & \cellcolor{color_3rd}{$2.45$} & \cellcolor{color_2nd}{$2.10$} & \cellcolor{color_1st}{$2.05$}\\
ALM & $3.57$ & \cellcolor{color_3rd}{$2.12$} & \cellcolor{color_4th}{$2.14$} &  \cellcolor{color_2nd}{$1.26$} & \cellcolor{color_1st}{$1.03$}\\
GDM & --- & \cellcolor{color_3rd}{$39.15$} & \cellcolor{color_2nd}{$28.20$} & \cellcolor{color_4th}{$45.15$} & \cellcolor{color_1st}{$4.04$}\\
VNC & $5.14$ & \cellcolor{color_3rd}{$4.47$} & \cellcolor{color_4th}{$4.64$} & \cellcolor{color_2nd}{$3.30$} & \cellcolor{color_1st}{$1.84$}\\
USQ & $13.54$ & \cellcolor{color_3rd}{$4.34$} & \cellcolor{color_4th}{$4.97$} & \cellcolor{color_2nd}{$3.83$} & \cellcolor{color_1st}{$3.77$}\\
ROF & \cellcolor{color_4th}{$2.11$} & \cellcolor{color_1st}{$1.59$} & \cellcolor{color_2nd}{$1.70$} & \cellcolor{color_3rd}{$1.85$} & $2.48$\\
{PIC} & $7.65$ & \cellcolor{color_2nd}{$2.38$} & \cellcolor{color_3rd}{$3.12$} & \cellcolor{color_1st}{$1.41$} & \cellcolor{color_4th}{$4.87$}\\
{TFG} & $13.20$ & \cellcolor{color_1st}{$1.85$} & \cellcolor{color_2nd}{$2.03$} & \cellcolor{color_3rd}{$2.63$} & \cellcolor{color_4th}{$4.88$}\\\Xhline{0.5pt}
{SNF} & $15.85$ & \cellcolor{color_2nd}{$3.05$} & \cellcolor{color_4th}{$3.56$} & \cellcolor{color_3rd}{$3.26$} & \cellcolor{color_1st}{$2.85$}\\\Xhline{1pt}
\end{tabular}
\label{tab3}
\end{table}
```

LaTeX简介

- Hello World

```
1  \documentclass{article}
2  \usepackage[utf8]{inputenc}
3
4  \title{test}
5  \author{xgao.nlpr }
6  \date{October 2021}
7
8  \begin{document}
9
10 \maketitle
11
12 \section{Introduction}
13
14 Hello World!
15
16 \end{document}
17
```

test

xgao.nlpr

October 2021

1 Introduction

Hello World!

- 用Overleaf新建一个空工程，进入工程并通过快捷键Ctrl+Enter进行编译
  - 第1行\documentclass{article} 文章（article）样式
  - \titile{}，\author{}，\date{}命令为标题信息命令，用于输入相关信息
  - \maketitile为制作标题页命令，用于显示标题相关信息

LaTeX简介

- Hello World

```
1  \documentclass{article}
2  \usepackage[utf8]{inputenc}
3
4  \title{test}
5  \author{xgao.nlpr }
6  \date{October 2021}
7
8  \begin{document}
9
10 \maketitle
11
12 \section{Introduction}
13
14 Hello World!
15
16 \end{document}
17
```

test

xgao.nlpr

October 2021

1 Introduction

Hello World!

- \usepackage[]{}为宏包加载命令，相当于C中的#include <>命令
- 正文位于\begin{document}与\end{document}之间，相当于C的main()函数
- 形如\command[]{}为排版命令，通常以“\”开头，相当于C中的函数，其可选项与参数分别置于“[]”与“{}”之间

课程简介

- 课程目标
  - 掌握LaTeX排版基本命令或其查找方式
  - 运用LaTeX在给定模板上进行论文排版

课程简介

- 课程目标
  - 掌握LaTeX排版基本命令或其查找方式
  - 运用LaTeX在给定模板上进行论文排版
- 参考书目
  - 简单高效LaTeX，吴康隆，人民邮电出版社，2020年7月第1版，GitHub
  - The Not So Short Introduction To LaTeX (Chinese Edition), v6.02，GitHub

模板示例

- IEEE Template Selector

- Springer International Journal of Computer Vision (IJCV)

MSWord: The journal does not provide MSWord templates for your manuscript. Please consult each section of the Instructions for Authors to ensure all components of your article have been properly included (references, table, figures, etc). If accepted, your article will be formatted by our production team.

模板示例

- IEEE Conference on Computer Vision and Pattern Recognition (CVPR)

  Papers are limited to eight pages, including figures and tables, in the CVPR style. detailed formatting instructions:

  - Example submission paper with detailed instructions
  - LaTeX/Word Templates (tar)
  - LaTeX/Word Templates (zip)

- ACM SIGGRAPH

Templates and Instructions

Authors who submit material to SIGGRAPH-sponsored events must use ACM's article template. The "acmsiggraph" template has been deprecated - please do not use it.

LaTeX and Microsoft Word templates for Windows and Macintosh (Office 2011, Office 2016) are available. The use of LaTeX is **strongly recommended** over Microsoft Word. The LaTeX template is distributed to major TeX repositories - you may find that it is already installed, or available via a package update on your computer (TeX Live 2016, MacTeX, MikTeX, etc.).

模板示例

- IEEE Signal Processing Letters (SPL) Manuscript

Hierarchical RANSAC-Based Rotation Averaging

Xiang Gao, Jiazheng Luo, Kunqian Li, and Zexiao Xie

***Abstract*—In this letter, we present a novel rotation averaging pipeline, which is performed in a hierarchical manner. Unlike the traditional rotation averaging methods which focus on designing robust loss function to get rid of the impacts of the relative rotation outliers, here the outliers are detected and filtered by leveraging the well-known robust model estimation procedure, RANdom SAmple Consensus (RANSAC). During the RANSAC process, the minimal set is randomly sampled by random tree spanning on the Epipolar-geometry Graph (EG). As the RANSAC estimation result is sensitive to the size of minimal set, the EG is clustered into several sub-graphs, and the inner- and inter-cluster RANSAC-based rotation averaging are performed hierarchically. In addition, both random generation and optimal selection of the minimal set are performed in a weighted manner to make the rotation averaging pipeline more robust. Ablation studies and comparison experiments on the 1DSfM and San Francisco (SNF) datasets demonstrate the effectiveness of our proposed method.**

***Index Terms*—Rotation averaging, random tree spanning, graph clustering, weighted selection and optimization.**

I. Introduction

ROTATION averaging [1] estimates the absolute camera orientations given the relative rotation measurements, which is a critical step in global Structure-from-Motion (SfM) methods [2], [3], [4], [5], [6]. Though has been widely investigated [7], [8], [9], [10], [11], the rotation averaging problem is far from being solved as the relative rotations in Epipolar-geometry Graph (EG) contain inevitable outliers, which are resulted from feature mis-matches, especially for the image collections downloaded from the Internet [12]. To deal with this issue, existing methods usually seek to design complicated loss functions to make the optimization process more robust to the relative rotation outliers [8], [9], [10], [11]. Though proven to be effective and integrated into several global SfM pipelines [2], [3], [4], [6], these methods heavily depend the initialization and sometimes even fall into local minima which would lead to poor rotation averaging results [13].

In contrast to the above methods, this letter presents a novel rotation averaging pipeline, which is concentrated on detecting and filtering the relative rotation outliers. Instead of introducing the commonly-used loop constraints [5], [14], [15], here the outliers are detected by the well-known robust model estimation procedure, RANdom SAmple Consensus (RANSAC) [16]. In order to perform a RANSAC-based rotation averaging, random spanning tree on the EG is involved, whose edges are served as the minimal set for model estimation and outlier detection. As we know, the result of RANSAC-based estimation is sensitive to the size and inlier ratio of the minimal set. To make our method more effective and robust, two strategies, including graph clustering and edge weighting, are adopted. For graph clustering, the EG is firstly clustered into several sub-graphs, and then the inner- and inter-cluster RANSAC-based rotation averaging are performed. For edge weighting, both random generation and optimal selection of the minimal set in our pipeline are performed in a weighted manner to increase the reliability of each RANSAC iteration and the whole RANSAC process.

The main contributions of this letter are three folds: 1) A novel RANSAC-like rotation averaging pipeline is presented, which is realized by random tree spanning; 2) Two key strategies, including graph clustering and edge weighting, are introduced to make our method more effective and robust; 3) Comparison experiments with several state of the arts on the well-known 1DSfM [2] and San Francisco (SNF) [9] datasets are performed to demonstrate the effectiveness and advantage of our proposed method.

Manuscript received September 3, 2020; revised October 6, 2020; accepted October 10, 2020. Date of publication Month Day, Year; date of current version Month Day, Year. This work is supported by the National Science Foundation of China (62003319, 62076026, and 61906177), the Open Projects Program of National Laboratory of Pattern Recognition (202000010), and the Post-Doctoral Applied Research Projects of Qingdao. *(Corresponding author: Kunqian Li.)*

X. Gao, J. Luo, K. Li, and Z. Xie are with College of Engineering, Ocean University of China, Qingdao 266100, China (e-mail: xgao@ouc.edu.cn; luojiazheng@stu.ouc.edu.cn; likunqian@ouc.edu.cn; xiezexiao@ouc.edu.cn).

II. Related Works

In this section, two main types of existing rotation averaging methods, including robust loss-based and outlier filtering-based ones, are briefly reviewed.

A. Robust loss-based rotation averaging

The robust loss-based rotation averaging methods [10], [11] seek to design loss functions to achieve robust estimations of the absolute rotations in the presence of the relative rotation outliers. Chatterjee *et al.* [10] developed a two-step rotation averaging method. They firstly used the ℓ_1 solution as an initialization to make their method robust to the relative rotation outliers. Then, an Iteratively Reweighted Least Squares (IRLS) approach was followed to achieve an efficient and accurate absolute rotation estimation. Chatterjee *et al.* extended their previous work in [11]. For the initialization step, ℓ_1-based optimization was still used. As for the IRLS step, they provided a fairly exhaustive evaluation of the performances of a variety of robust loss functions, and their evaluation led to a recommendation of the $\ell_{\frac{1}{2}}$ loss function. Though the above methods are robust to the relative rotation outliers to some extent, the optimization in these methods heavily depends on the initialization and sometimes it would fall into local minimum unexpectedly [13].

B. Outlier filtering-based rotation averaging

Compared with the robust loss-based rotation averaging methods, the outlier filtering-based ones [7], [17] are more

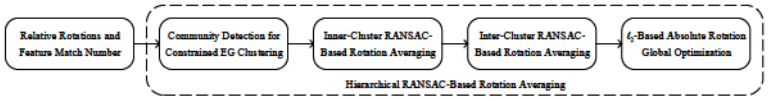

Fig. 1. Pipeline of our proposed hierarchical RANSAC-based rotation averaging. The input of our method is the relative rotations and the feature match number, $\{\boldsymbol{R}_{ij}, n_{ij} | e_{ij} \in \mathcal{E}\}$, between matched image pairs, and the output of our method is the optimized absolute rotation, $\{\boldsymbol{R}_i^* | v_i \in \mathcal{V}\}$, of each camera.

straightforward in principle. This type of methods follows the clean-then-optimize strategy, *i.e.* first clean the EG by detecting and filtering the relative rotation outliers and then optimize the cleaned EG using existing rotation averaging methods, *e.g.* [11]. Govindu [7] presented a primary research on the RANSAC-based rotation averaging method. It generated random spanning trees on the EG with random depth first search, which were used to initialize the absolute rotation estimations and detect the relative rotation outliers. Then the absolute rotations are optimized in an iterative manner. Cui *et al.* [17] proposed a multiple Orthogonal Maximum Spanning Trees (OMSTs)-based rotation averaging method. Based on the observation from statistical view that the relative rotation accuracy was positively correlated with the feature match number, they selected multiple OMSTs from the original EG to obtain a set of densely connected and more accurate relative rotations to upgrade the input of rotation averaging.

Though similar in principle, there are several differences between [7] and ours: 1) We present a novel random spanning tree approach in a weighted manner based on random breadth first search; 2) We perform graph clustering on the EG to downsize the minimal set and improve the method robustness; 3) We utilize the simple ℓ_2-based loss function for optimization as the absolute rotations are accurately and robustly initialized.

III. Preliminaries

In this section, several preliminaries of our work, including the definition of rotation averaging problem and the choices of loss function and distance measure, are briefly introduced.

Considering an EG, denoted as $\mathcal{G} = (\mathcal{V}, \mathcal{E})$, is formed by $|\mathcal{V}|$ cameras and $|\mathcal{E}|$ relative rotation measurements. A vertex $v_i \in \mathcal{V}$ corresponds to a camera with absolute rotation $\boldsymbol{R}_i$ and an edge $e_{ij} \in \mathcal{E}$ links an image pair with relative rotation $\boldsymbol{R}_{ij}$. Then, the rotation averaging problem is defined as:

$$\{\boldsymbol{R}_i^*\} = \arg\min \sum_{e_{ij} \in \mathcal{E}} \rho\left(d(\boldsymbol{R}_{ij}, \boldsymbol{R}_j \boldsymbol{R}_i^T)\right), \quad (1)$$

where $\{\boldsymbol{R}_i^*\}$ is the estimated absolute rotations, $\rho(.)$ is the loss function for robust optimization, and $d(.,.)$ is the distance measure between the measured and re-computed relative rotations. For loss function $\rho()$, thanks to our effective outlier filtering strategy, the simple ℓ_2 loss is used in this letter. For distance measure $d(.,.)$, we choose the angular distance $d_\theta(.,.)$, which is used in most of the related works [10], [11], [17], [18]. Based on the chosen distance measure, the inlier/outlier criterion is defined as follows: A relative rotation $\boldsymbol{R}_{ij}$ is an inlier if $d_\theta(\boldsymbol{R}_{ij}, \boldsymbol{R}_j^* (\boldsymbol{R}_i^*)^T) < \theta_{th}$, where θ_{th} is the angular distance threshold and is set to 3° in this letter.

IV. Proposed Method

In this section, our proposed hierarchical RANSAC-based rotation averaging method is described. The input of our method includes the relative rotations and feature match number between matched image pairs, which are denoted as $\{\boldsymbol{R}_{ij}, n_{ij} | e_{ij} \in \mathcal{E}\}$. The feature match number n_{ij} is used to weight the edges of EG as the accuracy of $\boldsymbol{R}_{ij}$ is positively correlated with n_{ij} statistically [17]. The output of our method is the optimized absolute rotation of each camera, which is denoted as $\{\boldsymbol{R}_i^* | v_i \in \mathcal{V}\}$. Fig. 1 shows the pipeline of our method: 1) A constrained community detection algorithm [19] is employed on the original EG to cluster it into several sub-graphs; 2) Inner- and inter-cluster RANSAC-based rotation averaging is performed successively for relative rotation outlier detection and absolute rotation estimation initialization; 3) ℓ_2-based global optimization is conducted on the basis of outlier detection and estimation initialization to obtain the final rotation averaging results. In the following, several key techniques of our proposed method are detailed.

A. Random Tree Spanning

RANSAC is known as a bottom-up methodology which performs several times of model estimation with randomly sampled minimal set, and the estimation result is set to the model with largest size of supporting set. For the rotation averaging problem, the minimal set consists of the edges of a spanning tree on the EG. As a result, random spanning tree is involved in our method for minimal set generation.

In this letter, the random tree is spanned based on the idea of breadth first search. Specifically, the tree spanning process starts from anyone of the EG vertices. Without loss of generality, the first vertex is used as the spanning origin. Suppose the current vertex set has (has not) been spanned is denoted as $\mathcal{V}_1(\mathcal{V}_2)$, and the edge set between $\mathcal{V}_1$ and $\mathcal{V}_2$ is denoted as $\mathcal{E}_{12}$. An edge is randomly selected from $\mathcal{E}_{12}$ and the unspanned vertex connected by the selected edge is moved from $\mathcal{V}_2$ to $\mathcal{V}_1$. The above random selection process is iterated until $\mathcal{V}_2$ becomes an empty set.

In addition, as the minimal set with all inliers is preferred for RANSAC procedure, the random tree is spanned in a weighted manner here. Specifically, suppose the number of feature matches of an edge $e_{ij} \in \mathcal{E}_{12}$ is denoted as n_{ij}, the probability of e_{ij} being selected from $\mathcal{E}_{12}$ is $P(e_{ij}) = \frac{n_{ij}}{\sum_{e_{ij} \in \mathcal{E}_{12}} n_{ij}}$.

B. RANSAC-based rotation averaging

After minimal set generation by random tree spanning, it is involved in the RANSAC process for absolute rotation

模板示例

- IEEE Signal Processing Letters (SPL) Manuscript

estimation. The initial estimation of each absolute rotation is obtained by firstly finding the paths between the fiducial and the other vertices, and then chaining the relative rotations along the paths. Based on the initial estimation, the supporting set of the random spanning tree could be obtained by:

$$\mathcal{E}^{\mathbb{S}} = \left\{ d_\theta(\boldsymbol{R}_{ij}, \boldsymbol{R}_j^\dagger (\boldsymbol{R}_i^\dagger)^T) < \theta_{th} | e_{ij} \in \mathcal{E} \right\}, \quad (2)$$

where $\{\boldsymbol{R}_i^\dagger\}$ is the initial estimation of each absolute rotation obtained from the random spanning tree and $\mathbb{S}$ denotes supporting. Generally, during the RANSAC process, several minimal sets, 100 in this letter, are randomly generated and the optimal one is the one with largest size of the supporting set $|\mathcal{E}^{\mathbb{S}}|$. Here, we consider the feature match number once again and the optimal minimal set is the one with largest sum of feature match number of its supporting set $\sum_{e_{ij} \in \mathcal{E}^{\mathbb{S}}} n_{ij}$.

Then, the absolute rotations are optimized by the following weighted ℓ_2-based optimization:

$$\{\boldsymbol{R}_i^\star\} = \arg\min \sum_{e_{ij} \in \mathcal{E}^{\mathbb{S}}} \left\| n_{ij} d_\theta(\boldsymbol{R}_{ij}, \boldsymbol{R}_j^\dagger (\boldsymbol{R}_i^\dagger)^T) \right\|_{\ell_2}. \quad (3)$$

C. Hierarchical rotation averaging

Theoretically, absolute rotations could be estimated by the above RANSAC-like rotation averaging pipeline based on weighted random tree spanning and ℓ_2-based optimization. However, it is almost impossible to generate a spanning tree on the entire EG with all inlier edges, especially for the large-scale image set. In order to improve the effectiveness and robustness of our rotation averaging method, a hierarchical rotation averaging pipeline is proposed. The original EG is firstly clustered into several sub-graphs. Then, rotation averaging is performed in a hierarchical manner, including inner- and inter-cluster RANSAC-based rotation averaging, and ℓ_2-based absolute rotation global optimization.

Community detection for constrained EG clustering: Graph clustering has been widely investigated in recent years [20], [21], [22]. Here we choose the Louvain's algorithm-based community detection methods [23], [24] for EG clustering, which are also used in [18], [19], [25], [26]. In addition, as the RANSAC-based rotation averaging is sensitive to the size of the minimal set, here the EG is clustered in a constrained way [19], *i.e.* constraining the max size of each cluster to a pre-set upper limit, 100 in this letter. The influence of the max cluster size is discussed in the supplemental text material.

Inner-cluster RANSAC-based rotation averaging: After graph clustering, each cluster is with less vertices and edges. Then, the RANSAC-based rotation averaging is performed on each cluster individually. This is the low-level step in our hierarchical pipeline. Note that the rotation averaging results are in their local coordinate systems for all clusters.

Inter-cluster RANSAC-based rotation averaging: By considering each cluster (including the vertices and edges in the cluster) as a vertex and the edges between two clusters as an edge, the cluster-based structure could be regarded as a high-level graph, and the absolute rotations of all the cluster local coordinate systems could also be estimated by the RANSAC-based rotation averaging method. This is the high-level step in our hierarchical pipeline. After the above low- and high-level steps, all the clusters, including the vertices in them, are aligned into a uniform global coordinate system.

However, for the inter-cluster RANSAC-based rotation averaging, there are usually many edges between two clusters connecting different vertices. In order to perform the high-level rotation averaging, we need to obtain the relative rotation between the local coordinate systems of the cluster pair from these inter-cluster edges. Suppose after inner-cluster RANSAC-based rotation averaging, the absolute rotations of the m-th cluster are denoted as $\{\boldsymbol{R}_m^i | v_m^i \in \mathcal{V}_m\}$ and the relative rotations of the edges between the m-th and the n-th clusters are denoted as $\{\boldsymbol{R}_{mn}^{ij} | e_{mn}^{ij} \in \mathcal{E}_{mn}\}$. For each relative rotation in $\{\boldsymbol{R}_{mn}^{ij}\}$, an estimation of the relative rotation between the m-th and the n-th clusters could be obtained by:

$$\widetilde{\boldsymbol{R}}_{mn}^{ij} = (\boldsymbol{R}_n^j)^T \boldsymbol{R}_{mn}^{ij} \boldsymbol{R}_m^i. \quad (4)$$

Note that the local coordinate system of each cluster is constructed on the first vertex of the cluster in this letter.

Theoretically, all the rotations in $\{\widetilde{\boldsymbol{R}}_{mn}^{ij}\}$ should be identical as all of them represent the relative rotation between the cluster pair. However, that is impossible due to the inevitable estimation errors in $\{\boldsymbol{R}_m^i\}$, $\{\boldsymbol{R}_n^j\}$, and $\{\boldsymbol{R}_{mn}^{ij}\}$. As a result, the problem of inter-cluster relative rotation estimation problem is boiled down to a single rotation averaging problem [1], *i.e.* averaging to give the best rotation from several estimations of a single rotation. This problem is solved by a RANSAC-like approach again in this letter, which is detailed in the following.

For each RANSAC iteration, a rotation $\boldsymbol{R}_{mn}^\dagger$ is randomly sampled from the inter-cluster relative rotation set $\{\widetilde{\boldsymbol{R}}_{mn}^{ij}\}$ in a weighted manner and its supporting set is obtained by:

$$\mathcal{E}_{mn}^{\mathbb{S}} = \left\{ d_\theta(\widetilde{\boldsymbol{R}}_{mn}^{ij}, \boldsymbol{R}_{mn}^\dagger) < \theta_{th} | e_{mn}^{ij} \in \mathcal{E}_{mn} \right\}. \quad (5)$$

Similar to our RANSAC-based multiple rotation averaging method, the optimal minimal set, here a single rotation, is the one with largest sum of feature match number of its supporting set $\sum_{e_{mn}^{ij} \in \mathcal{E}_{mn}^{\mathbb{S}}} n_{mn}^{ij}$ among all the 100 randomly selected single rotations in this letter.

Then, the inter-cluster relative rotation is also optimized by a weighted ℓ_2-based optimization:

$$\boldsymbol{R}_{mn}^\star = \arg\min \sum_{e_{mn}^{ij} \in \mathcal{E}_{mn}^{\mathbb{S}}} \left\| n_{mn}^{ij} d_\theta(\widetilde{\boldsymbol{R}}_{mn}^{ij}, \boldsymbol{R}_{mn}^\dagger) \right\|_{\ell_2}. \quad (6)$$

ℓ_2-based absolute rotation global optimization: On the basis of the inner- and inter-cluster RANSAC-based rotation averaging, the absolute rotations of the vertices have been initialized and the relative rotation outliers of the edges have been detected. Then, a weighted ℓ_2-based global optimization, which is similar to that of Eq. 3, is performed on the cleaned EG to optimize all the absolute rotations, by which the final rotation averaging result is achieved.

V. Evaluation

In this section, our proposed hierarchical RANSAC-based rotation averaging method is comprehensively evaluated. We first introduce the data and measure for method evaluation. On this basis, ablation studies and comparison experiments with several state of the arts are performed.

TABLE I
META-DATA OF THE EVALUATION DATASETS.

Data	$\lvert\mathcal{V}\rvert(\lvert\mathcal{V}_{gt}\rvert)$	$\lvert\mathcal{E}\rvert$	$\lvert\mathcal{C}\rvert$	$\bar{r}_{ij}$	$\tilde{r}_{ij}$	$\bar{n}_{ij}$	$\tilde{n}_{ij}$
ELS	247(227)	20297	5	2.89	12.50	106	160
PDP	354(338)	24710	6	1.81	8.38	87	128
NYC	376(332)	20680	5	4.22	14.14	80	167
MDR	394(341)	23784	6	9.34	29.30	61	128
YKM	458(437)	27729	7	2.68	11.16	112	245
MND	474(450)	52424	7	1.67	7.51	180	310
TOL	508(472)	23863	7	2.60	11.58	81	220
ALM	627(577)	97206	7	2.78	9.09	105	192
GDM	742(677)	48144	11	12.30	33.33	73	144
VNC	918(836)	103550	13	2.59	11.26	229	408
USQ	930(789)	25561	13	3.61	9.02	87	150
ROF	1134(1084)	70187	12	2.97	13.83	65	188
PIC	2508(2152)	319257	29	4.93	19.09	56	97
TFG	5433(5058)	680012	58	3.01	8.62	71	109
SNF	7866(7866)	101512	101	0.99	1.81	107	153

TABLE II
ABLATION STUDY RESULTS ON THE EVALUATION DATASETS.

Data	Without weighting	Without clustering	Without constraint	Without optimizing	Proposed method
ELS	0.97	1.32	0.60	2.23	0.59
PDP	1.24	1.48	0.95	2.22	0.92
NYC	2.45	4.51	1.32	3.09	1.24
MDR	9.31	35.38	1.47	6.98	2.54
YKM	1.95	2.90	1.72	2.87	1.57
MND	0.74	1.03	0.53	1.77	0.62
TOL	2.17	4.08	2.47	3.40	2.05
ALM	1.21	2.11	1.11	2.34	1.03
GDM	21.18	21.26	3.91	13.36	4.04
VNC	2.50	3.63	1.86	4.14	1.84
USQ	5.31	15.35	5.35	7.51	3.77
ROF	5.97	10.55	2.27	6.01	2.48
PIC	19.44	14.45	11.53	10.33	4.87
TFG	17.54	13.25	5.94	15.62	4.88
SNF	5.52	15.07	3.79	6.63	2.85

A. Data and Measure

The evaluation is performed on the 1DSfM [2] and SNF [9] datasets. The 1DSfM dataset contains images of 14 scenes downloaded from the Internet while the SNF dataset contains 7866 Google Street View images. The relative rotations and feature match number between image pairs of each test data are also provided. The meta-data of the evaluation datasets is listed in Table I. The number in the round bracket indicates the number of vertices with ground truths $\mathcal{V}_{gt}$. $|\mathcal{C}|$ denotes the number of clusters obtained by the constrained EG clustering. $\bar{r}_{ij}$ and $\tilde{r}_{ij}$ are the median and mean errors of relative rotations, and $\bar{n}_{ij}$ and $\tilde{n}_{ij}$ are the median and mean values of feature match number. To evaluate the rotation averaging accuracy, the estimated absolute rotations are aligned to the ground truths with a best relative rotation between the two rotation sets [10], [11]. Then, the median value of the alignment errors is used as the accuracy evaluation measure [8], [10], [11].

B. Ablation studies

Ablation studies are conducted to demonstrate the effectiveness of our proposed method, which are briefly introduced.

Without weighting: In this situation, all edges are identically treated during the rotation averaging process, *i.e.* n_{ij} is not involved in minimal set selection or ℓ_2-based optimization.

Without clustering: In this situation, community detection for EG clustering is not performed, and the RANSAC-based rotation averaging method is conducted on the entire EG.

TABLE III
COMPARISON EXPERIMENT RESULTS ON THE EVALUATION DATASETS.

Data	Weiszfeld [8]	ℓ_1-IRLS [10]	$\ell_{\frac{1}{2}}$-IRLS [11]	OMSTs [17]	Proposed method
ELS	1.66	1.02	1.15	0.75	0.59
PDP	3.35	2.19	2.62	1.73	0.92
NYC	2.43	1.43	1.40	1.30	1.24
MDR	4.37	2.75	3.08	1.12	2.54
YKM	2.73	1.71	1.62	1.55	1.57
MND	0.92	0.77	0.71	0.68	0.62
TOL	2.73	2.55	2.45	2.10	2.05
ALM	3.57	2.12	2.14	1.26	1.03
GDM	—	39.15	28.20	45.15	4.04
VNC	5.14	4.47	4.64	3.30	1.84
USQ	13.54	4.34	4.97	3.83	3.77
ROF	2.11	1.59	1.70	1.85	2.48
PIC	7.65	2.38	3.12	1.41	4.87
TFG	13.20	1.85	2.03	2.63	4.88
SNF	15.85	3.05	3.56	3.26	2.85

Without constraint: In this situation, the EG is clustered using the unconstrained Louvain's algorithm, *i.e.* the EG is clustered without setting the max size of each cluster.

Without optimizing: In this situation, neither the final global optimization nor the optimization in inner- or inter-cluster RANSAC-based rotation averaging is performed.

The ablation study results are shown in Table II. We can see that the rotation averaging accuracies have obvious decreases in most ablation study situations compared with our proposed method. As a result, all the strategies of edge weighting, (constrained) graph clustering, and ℓ_2-based optimization could increase the accuracy and robustness of our method. Note that the method of [7] could be approximately considered as our proposed method with neither weighting nor clustering.

C. Comparison experiments

Comparison experiments are performed between our proposed method and several state-of-the-art rotation averaging methods, including Weiszfeld [8], ℓ_1-IRLS [10], ℓ_1-IRLS($\ell_{\frac{1}{2}}$) [11], and OMSTs [17]. The comparison experiment results are shown in Table III. We can see that our proposed method achieves the overall best performance among all the comparative methods: It achieves best results on 10 test data and second-best results on 2 test data among all 15 test data. Though our proposed method does not perform very well on three relatively larger-scale test data, ROF, PIC, and TFG, we believe that not only the data size, but also some other data characteristics, *e.g.* noise level and connectivity tightness of the EG, would influence its result [27], as the best result is also achieved by our proposed method on the largest test data, SNF.

VI. Conclusion

This letter presents a hierarchical RANSAC-based rotation averaging pipeline to deal with the relative rotation outliers. The absolute rotations are initialized by random tree spanning on the EG and are optimized with the supporting set of the optimal random spanning tree. Besides, two key strategies, including graph clustering and edge weighting, are involved to make our method more effective and robust. Ablation studies and comparison experiments on the 1DSfM and SNF datasets demonstrate the effectiveness of our proposed method.

模板示例

- IEEE Signal Processing Letters (SPL) Manuscript

REFERENCES

[1] R. Hartley, J. Trumpf, Y. Dai, and H. Li, "Rotation averaging," *International Journal of Computer Vision*, vol. 103, p. 267–305, 2013.

[2] K. Wilson and N. Snavely, "Robust global translations with 1DSfM," in *European Conference on Computer Vision (ECCV)*, 2014, pp. 61–75.

[3] Z. Cui and P. Tan, "Global structure-from-motion by similarity averaging," in *IEEE International Conference on Computer Vision (ICCV)*, 2015, pp. 864–872.

[4] O. Özyeşil and A. Singer, "Robust camera location estimation by convex programming," in *IEEE Conference on Computer Vision and Pattern Recognition (CVPR)*, 2015, pp. 2674–2683.

[5] C. Sweeney, T. Sattler, T. Höllerer, M. Turk, and M. Pollefeys, "Optimizing the viewing graph for structure-from-motion," in *IEEE International Conference on Computer Vision (ICCV)*, 2015, pp. 801–809.

[6] Q. Dong, X. Gao, H. Cui, and Z. Hu, "Robust camera translation estimation via rank enforcement," *IEEE Transactions on Cybernetics*, 2020.

[7] V. M. Govindu, "Robustness in motion averaging," in *Asian Conference on Computer Vision (ACCV)*, 2006, pp. 457–466.

[8] R. Hartley, K. Aftab, and J. Trumpf, "L1 rotation averaging using the Weiszfeld algorithm," in *IEEE Conference on Computer Vision and Pattern Recognition (CVPR)*, 2011, pp. 3041–3048.

[9] D. Crandall, A. Owens, N. Snavely, and D. Huttenlocher, "SfM with MRFs: Discrete-continuous optimization for large-scale structure from motion," *IEEE Transactions on Pattern Analysis and Machine Intelligence*, vol. 35, no. 12, pp. 2841–2853, 2013.

[10] A. Chatterjee and V. M. Govindu, "Efficient and robust large-scale rotation averaging," in *IEEE International Conference on Computer Vision (ICCV)*, 2013, pp. 521–528.

[11] A. Chatterjee and V. M. Govindu, "Robust relative rotation averaging," *IEEE Transactions on Pattern Analysis and Machine Intelligence*, vol. 40, no. 4, pp. 958–972, 2018.

[12] N. Snavely, S. M. Seitz, and R. Szeliski, "Modeling the world from Internet photo collections," *International Journal of Computer Vision*, vol. 80, no. 2, pp. 189–210, 2008.

[13] K. Wilson and D. Bindel, "On the distribution of minima in intrinsic-metric rotation averaging," in *IEEE/CVF Conference on Computer Vision and Pattern Recognition (CVPR)*, 2020, pp. 6030–6038.

[14] C. Zach, M. Klopschitz, and M. Pollefeys, "Disambiguating visual relations using loop constraints," in *IEEE Conference on Computer Vision and Pattern Recognition (CVPR)*, 2010, pp. 1426–1433.

[15] N. Jiang, Z. Cui, and P. Tan, "A global linear method for camera pose registration," in *IEEE International Conference on Computer Vision (ICCV)*, 2013, pp. 481–488.

[16] M. A. Fischler and R. C. Bolles, "Random sample consensus: A paradigm for model fitting with applications to image analysis and automated cartography," *Communications of the ACM*, vol. 24, no. 6, pp. 381–395, 1981.

[17] H. Cui, S. Shen, W. Gao, H. Liu, and Z. Wang, "Efficient and robust large-scale structure-from-motion via track selection and camera prioritization," *ISPRS Journal of Photogrammetry and Remote Sensing*, vol. 156, pp. 202–214, 2019.

[18] T. Shen, S. Zhu, T. Fang, R. Zhang, and L. Quan, "Graph-based consistent matching for structure-from-motion," in *European Conference on Computer Vision (ECCV)*, 2016, pp. 139–155.

[19] L. Zhou, Z. Luo, M. Zhen, T. Shen, S. Li, Z. Huang, T. Fang, and L. Quan, "Stochastic bundle adjustment for efficient and scalable 3D reconstruction," in *European Conference on Computer Vision (ECCV)*, 2020.

[20] I. S. Dhillon, Y. Guan, and B. Kulis, "Weighted graph cuts without eigenvectors: A multilevel approach," *IEEE Transactions on Pattern Analysis and Machine Intelligence*, vol. 29, no. 11, pp. 1944–1957, 2007.

[21] Z. Kang, L. Wen, W. Chen, and Z. Xu, "Low-rank kernel learning for graph-based clustering," *Knowledge-Based Systems*, vol. 163, pp. 510 – 517, 2019.

[22] Z. Kang, H. Pan, S. C. H. Hoi, and Z. Xu, "Robust graph learning from noisy data," *IEEE Transactions on Cybernetics*, vol. 50, no. 5, pp. 1833–1843, 2020.

[23] M. E. J. Newman and M. Girvan, "Finding and evaluating community structure in networks," *Physical Review E*, vol. 69, p. 026113, 2004.

[24] V. D. Blondel, J.-L. Guillaume, R. Lambiotte, and E. Lefebvre, "Fast unfolding of communities in large networks," *Journal of Statistical Mechanics: Theory and Experiment*, vol. 2008, no. 10, p. P10008, 2008.

[25] H. Cui, X. Gao, S. Shen, and Z. Hu, "HSfM: Hybrid structure-from-motion," in *IEEE Conference on Computer Vision and Pattern Recognition (CVPR)*, 2017, pp. 2393–2402.

[26] H. Cui, S. Shen, X. Gao, and Z. Hu, "CSfM: Community-based structure from motion," in *IEEE International Conference on Image Processing (ICIP)*, 2017, pp. 4517–4521.

[27] K. Wilson, D. Bindel, and N. Snavely, "When is rotations averaging hard?" in *European Conference on Computer Vision (ECCV)*, 2016, pp. 255–270.

Supplemental Text Material for "Hierarchical RANSAC-Based Rotation Averaging"

Xiang Gao, Jiazheng Luo, Kunqian Li, and Zexiao Xie

TABLE IV
INFLUENCE OF THE MAX CLUSTER SIZE, WHERE Γ, $|\mathcal{C}|$, AND $\bar{\epsilon}$ DENOTE MAX CLUSTER SIZE, EG CLUSTER NUMBER, AND ROTATION AVERAGING ACCURACY RESPECTIVELY.

Γ / Data	1		50		100		200		∞	
	$\lvert\mathcal{C}\rvert$	$\bar{\epsilon}$	$\lvert\mathcal{C}\rvert$	$\bar{\epsilon}$	$\lvert\mathcal{C}\rvert$	$\bar{\epsilon}$	$\lvert\mathcal{C}\rvert$	$\bar{\epsilon}$	$\lvert\mathcal{C}\rvert$	$\bar{\epsilon}$
ELS	247	1.32	6	0.60	5	0.59	4	0.63	2	0.60
PDP	354	1.48	9	0.94	6	0.92	5	0.98	4	0.95
NYC	376	4.51	11	1.28	5	1.24	4	1.29	3	1.32
MDR	394	35.38	11	2.66	6	2.54	3	2.24	2	1.47
YKM	458	2.90	11	1.63	7	1.57	5	1.59	3	1.72
MND	474	1.03	12	0.61	7	0.62	4	0.60	3	0.53
TOL	508	4.08	14	1.98	7	2.05	5	2.27	4	2.47
ALM	627	2.11	14	1.12	7	1.03	6	1.09	3	1.11
GDM	742	21.26	18	4.01	11	4.04	6	4.17	4	3.91
VNC	918	3.63	23	1.85	13	1.84	9	1.87	4	1.86
USQ	930	15.35	25	3.83	13	3.77	7	3.75	5	5.35
ROF	1134	10.55	27	2.63	12	2.48	7	2.52	4	2.27
PIC	2508	14.45	51	5.77	29	4.87	18	4.53	4	11.53
TFG	5433	13.25	113	5.29	58	4.88	32	4.91	3	5.94
SNF	7866	15.07	184	2.89	101	2.85	56	2.91	7	3.79

This supplemental text material mainly discusses the influence of the max cluster size in the constrained EG clustering to the final rotation averaging results of our proposed method.

We perform our proposed rotation averaging method with 5 different max cluster sizes, which are $\Gamma = 1, 50, 100, 200, \infty$. Here, $\Gamma = 1$ means that each camera forms a cluster, *i.e.* the situation of **without clustering** in the ablation studies of the main text; And, $\Gamma = \infty$ means the EG clustering is not constrained, *i.e.* the situation of **without constraint** in the ablation studies of the main text. Similar to the main text, the experiments are also performed on the 1DSfM and SNF datasets, and the results are shown in Table IV.

From the Table we can see that: 1) The number of clusters $|\mathcal{C}|$ is positively correlated to the vertex number $|\mathcal{V}|$, and negatively correlated to the max cluster size Γ; 2) Our proposed method overall achieves better performance when Γ is set to moderate values, *i.e.* $\Gamma = 50, 100, 200$, than the extreme situations, *i.e.* $\Gamma = 1, \infty$, and the variation of Γ in a proper range would not much influence the final accuracy. The above observation comes to a conclusion that the specific value of Γ is not very important when it is in a proper range, but the involvement of (constrained) EG clustering or not is of much significance, which leads to the parameter setting of Γ to 100 in this letter.

In addition, the situation of $\Gamma = \infty$ achieves best performance on 4 text data, MDR, MND, GDM, and ROF. As the graph clustering result heavily depends on the graph structure, compared with the unconstrained one, the constrained EG clustering is likely to weaken the inner- or inter-connectivity of the clusters and worsen the rotation averaging results on MDR, MND, GDM, and ROF.

模板示例

- IEEE Signal Processing Letters (SPL) Manuscript

D:\Papers\personal\submission manuscripts\RANSAC RA\IEEEtran\IEEEtran\final\Mamuscript.tex - Sublime Text (UNREGISTERED)

File Edit Selection Find View Goto Tools Project Preferences Help

bib-file.bib | Mamuscript.tex | Supplementary.tex

```
\documentclass[letterpaper]{IEEEtran}
\ifCLASSINFOpdf
\else
\fi
\usepackage{times}
\usepackage{epsfig}
\usepackage{graphicx}
\usepackage{bm}
\usepackage{amsthm,amsmath,amssymb}
\usepackage{mathrsfs}
\usepackage{tabu}
\usepackage{multirow}
\usepackage{gensymb}
\usepackage{verbatim}
\usepackage{balance}
\usepackage{colortbl}
\usepackage{makecell}
\hyphenation{op-tical net-works semi-conduc-tor}

\definecolor{color_1st}{rgb}{1.0, 0.0, 1.0}
\definecolor{color_2nd}{rgb}{1.0, 0.4, 1.0}
\definecolor{color_3rd}{rgb}{1.0, 0.7, 1.0}
\definecolor{color_4th}{rgb}{1.0, 0.9, 1.0}

\begin{document}
\title{Hierarchical RANSAC-Based Rotation Averaging}
\author{Xiang-Gao, Jiazheng-Luo, Kunqian-Li, and Zexiao Xie
\thanks{Manuscript received September 3, 2020; revised October 6, 2020; accepted October 10, 2020. Date of publication Month Day, Year; date of current version Month Day, Year. This work is supported by the National Science Foundation of China (62003319, 62076026, and 61906177), the Open Projects Program of National Laboratory of Pattern Recognition (202000010), and the Post-Doctoral Applied Research Projects of Qingdao. \emph{(Corresponding author: Kunqian Li.)}}
\thanks{X. Gao, J. Luo, K. Li, and Z. Xie are with College of Engineering, Ocean University of China, Qingdao 266100, China (e-mail: xgao@ouc.edu.cn; luojiazheng@stu.ouc.edu.cn; likunqian@ouc.edu.cn; xiezexiao@ouc.edu.cn).}

\markboth{IEEE Signal Processing Letters,~Vol.~XX, No.~XX, Month~Year}
{IEEE Signal Processing Letters,~Vol.~XX, No.~XX, Month~Yearg}
\maketitle

\begin{abstract}
In this letter, we present a novel rotation averaging pipeline, which is performed in a hierarchical manner. Unlike the traditional rotation averaging methods which focus on designing robust loss function to get rid of the impacts of the relative rotation outliers, here the outliers are detected and filtered by leveraging the well-known robust model estimation procedure, RANdom SAmple Consensus (RANSAC). During the RANSAC process, the minimal set is randomly sampled by random tree spanning on the Epipolar-geometry Graph (EG). As the RANSAC estimation result is sensitive to the size of minimal set, the EG is clustered into several sub-graphs, and the inner- and inter-cluster RANSAC-based rotation averaging are performed hierarchically. In addition, both random generation and optimal selection of the minimal set are performed in a weighted manner to make the rotation averaging pipeline more robust. Ablation studies and comparison experiments on the 1DSfM and {San Francisco (SNF) datasets} demonstrate the effectiveness of our proposed method.
\end{abstract}

\begin{IEEEkeywords}
Rotation averaging, random tree spanning, graph clustering, weighted selection and optimization.
\end{IEEEkeywords}

\IEEEpeerreviewmaketitle

\section{Introduction}
\IEEEPARstart{R}{otation} averaging \cite{Hartley-IJCV-13} estimates the absolute camera orientations given the relative rotation measurements, which is a critical step in global Structure-from-Motion (SfM) methods \cite{Wilson-ECCV-14, Cui-ICCV-15, Ozyesil-CVPR-15, Sweeney-ICCV-15, Dong-TCYB-20}. Though has been widely investigated \cite{Govindu-ACCV-06, Hartley-CVPR-11, Crandall-TPAMI-13, Chatterjee-ICCV-13, Chatterjee-TPAMI-18}, the rotation averaging problem is far from being solved as the relative rotations in Epipolar-geometry Graph (EG) contain inevitable outliers, which are resulted from feature mis-matches, especially for the image collections downloaded from the Internet \cite{Snavely-IJCV-08}. To deal with this issue, existing methods usually seek to design complicated loss functions to make the optimization process more robust to the relative rotation outliers \cite{Hartley-CVPR-11, Crandall-TPAMI-13, Chatterjee-ICCV-13, Chatterjee-TPAMI-18}. Though proven to be effective and integrated into several global SfM pipelines \cite{Wilson-ECCV-14, Cui-ICCV-15, Ozyesil-CVPR-15, Dong-TCYB-20}, these methods heavily depend the initialization and sometimes even fall into local minima which would lead to poor rotation averaging results \cite{Wilson-CVPR-20}.

In contrast to the above methods, this letter presents a novel rotation averaging pipeline, which is concentrated on detecting and filtering the relative rotation outliers. Instead of introducing the commonly-used loop constraints \cite{Sweeney-ICCV-15, Zach-CVPR-10, Jiang-ICCV-13}, here the outliers are detected by the well-known robust model estimation procedure, RANdom SAmple Consensus (RANSAC) \cite{Fischler-CACM-81}. In order to perform a RANSAC-based rotation averaging, random spanning tree on the EG is involved, whose edges are served as the minimal set for model estimation and outlier detection. As we know, the result of RANSAC-based estimation is sensitive to the size and inlier ratio of the minimal set. To make our method more effective and robust, two strategies, including graph clustering and edge weighting, are adopted. For graph clustering, the EG is firstly clustered into several sub-graphs, and then the inner- and inter-cluster RANSAC-based rotation averaging are performed. For edge weighting, both random generation and optimal selection of the minimal set in our pipeline are performed in a weighted manner to increase the reliability of each RANSAC iteration and the whole RANSAC process.

The main contributions of this letter are three folds: 1)~A novel RANSAC-like rotation averaging pipeline is presented, which is realized by random tree spanning; 2)~Two key strategies, including graph clustering and edge weighting, are introduced to make our method more effective and robust; 3)~Comparison experiments with several state of the arts on the well-known 1DSfM \cite{Wilson-ECCV-14} and {San Francisco (SNF) \cite{Crandall-TPAMI-13} datasets} are performed to demonstrate the effectiveness and advantage of our proposed method.

\section{Related works}

In this section, two main types of existing rotation averaging methods, including robust loss-based and outlier filtering-based ones, are briefly reviewed.

\subsection{Robust loss-based rotation averaging}

The robust loss-based rotation averaging methods \cite{Chatterjee-ICCV-13, Chatterjee-TPAMI-18} seek to design loss functions to achieve robust estimations of the absolute rotations in the presence of the relative rotation outliers. Chatterjee \emph{et al.} \cite{Chatterjee-ICCV-13} developed a two-step rotation averaging method. They firstly used the $\ell_1$ solution as an initialization to make their method robust to the relative rotation outliers. Then, an Iteratively Reweighted Least Squares (IRLS) approach was followed to achieve
```

Line 1, Column 1 Tab Size: 4 LaTeX

模板示例

- IEEE Signal Processing Letters (SPL) Manuscript

D:\Papers\personal\submission manuscripts\RANSAC RA\IEEEtran\IEEEtran\final\Supplementary\Supplementary.tex - Sublime Text (UNREGISTERED)

File Edit Selection Find View Goto Tools Project Preferences Help

bib-file.bib | Mamuscript.tex | Supplementary.tex

```
\documentclass[letterpaper,onecolumn]{IEEEtran}
\ifCLASSINFOpdf
\else
\fi
\usepackage{times}
\usepackage{graphicx}
\usepackage{bm}
\usepackage{amsthm,amsmath,amssymb}
\usepackage{mathrsfs}
\usepackage{tabu}
\usepackage{multirow}
\usepackage{gensymb}
\usepackage{verbatim}
\usepackage{balance}
\usepackage{colortbl}
\usepackage{makecell}
\usepackage{diagbox}
\hyphenation{op-tical net-works semi-conduc-tor}

\definecolor{color_1st}{rgb}{1.0, 0.0, 1.0}
\definecolor{color_2nd}{rgb}{1.0, 0.4, 1.0}
\definecolor{color_3rd}{rgb}{1.0, 0.7, 1.0}
\definecolor{color_4th}{rgb}{1.0, 0.9, 1.0}

\setcounter{table}{3}

\begin{document}
\title{Supplemental Text Material for\\``Hierarchical RANSAC-Based Rotation Averaging''}
\author{Xiang-Gao, Jiazheng-Luo, Kunqian-Li, and Zexiao Xie}

\maketitle
\thispagestyle{empty}

\begin{table*}[!htb]
\centering
\caption{Influence of the max cluster size, where $\varGamma$, $|\mathcal{C}|$, and $\tilde{e}$ denote max cluster size,\\EG cluster number, and rotation averaging accuracy respectively.}
\begin{tabular}{l|cc|cc|cc|cc}\Xhline{1pt}
\multirow{2}{*}{\diagbox{Data}{$\varGamma$}} & \multicolumn{2}{c|}{$1} & \multicolumn{2}{c|}{$50} & \multicolumn{2}{c|}{$100} & \multicolumn{2}{c}{$200} & \multicolumn{2}{c}{$\infty$}\\\cline{2-11}
 & $|\mathcal{C}|$ & $\tilde{e}$ & $|\mathcal{C}|$ & $\tilde{e}$ & $|\mathcal{C}|$ & $\tilde{e}$ & $|\mathcal{C}|$ & $\tilde{e}$ & $|\mathcal{C}|$ & $\tilde{e}$\\\hline
ELS & $247$ & $1.32$ & $6$ & \cellcolor{color_2nd}{$0.60$} & $5$ & \cellcolor{color_1st}{$0.59$} & $4$ & \cellcolor{color_4th}{$0.63$} & $2$ & \cellcolor{color_2nd}{$0.60$}\\
PDP & $354$ & $1.48$ & $9$ & \cellcolor{color_2nd}{$0.94$} & $6$ & \cellcolor{color_1st}{$0.92$} & $5$ & \cellcolor{color_4th}{$0.98$} & $4$ & \cellcolor{color_3rd}{$0.95$}\\
NYC & $376$ & $4.51$ & $11$ & \cellcolor{color_2nd}{$1.28$} & $5$ & \cellcolor{color_1st}{$1.24$} & $4$ & \cellcolor{color_3rd}{$1.29$} & $3$ & \cellcolor{color_4th}{$1.32$}\\
MDR & $394$ & $35.38$ & $11$ & \cellcolor{color_4th}{$2.66$} & $6$ & \cellcolor{color_3rd}{$2.54$} & $3$ & \cellcolor{color_2nd}{$2.24$} & $2$ & \cellcolor{color_1st}{$1.47$}\\
YKM & $458$ & $2.90$ & $11$ & \cellcolor{color_3rd}{$1.63$} & $7$ & \cellcolor{color_1st}{$1.57$} & $5$ & \cellcolor{color_2nd}{$1.59$} & $3$ & \cellcolor{color_4th}{$1.72$}\\
MND & $474$ & $1.03$ & $12$ & \cellcolor{color_3rd}{$0.61$} & $7$ & \cellcolor{color_4th}{$0.62$} & $4$ & \cellcolor{color_2nd}{$0.60$} & $3$ & \cellcolor{color_1st}{$0.53$}\\
TOL & $508$ & $4.08$ & $14$ & \cellcolor{color_1st}{$1.98$} & $7$ & \cellcolor{color_2nd}{$2.05$} & $5$ & \cellcolor{color_3rd}{$2.27$} & $4$ & \cellcolor{color_4th}{$2.47$}\\
ALM & $627$ & $2.11$ & $14$ & \cellcolor{color_4th}{$1.12$} & $7$ & \cellcolor{color_1st}{$1.03$} & $6$ & \cellcolor{color_2nd}{$1.09$} & $3$ & \cellcolor{color_3rd}{$1.11$}\\
GDM & $742$ & $21.26$ & $18$ & \cellcolor{color_2nd}{$4.01$} & $11$ & \cellcolor{color_3rd}{$4.04$} & $6$ & \cellcolor{color_4th}{$4.17$} & $4$ & \cellcolor{color_1st}{$3.91$}\\
VNC & $918$ & $3.63$ & $23$ & \cellcolor{color_2nd}{$1.85$} & $13$ & \cellcolor{color_1st}{$1.84$} & $9$ & \cellcolor{color_4th}{$1.87$} & $4$ & \cellcolor{color_3rd}{$1.86$}\\
USQ & $930$ & $15.35$ & $25$ & \cellcolor{color_3rd}{$3.83$} & $13$ & \cellcolor{color_2nd}{$3.77$} & $7$ & \cellcolor{color_1st}{$3.75$} & $5$ & \cellcolor{color_4th}{$5.35$}\\
ROF & $1134$ & $10.55$ & $27$ & \cellcolor{color_4th}{$2.63$} & $12$ & \cellcolor{color_2nd}{$2.48$} & $7$ & \cellcolor{color_3rd}{$2.52$} & $4$ & \cellcolor{color_1st}{$2.27$}\\
PIC & $2508$ & $14.45$ & $51$ & \cellcolor{color_3rd}{$5.77$} & $29$ & \cellcolor{color_2nd}{$4.87$} & $18$ & \cellcolor{color_1st}{$4.53$} & $4$ & \cellcolor{color_4th}{$11.53$}\\
TFG & $5433$ & $13.25$ & $113$ & \cellcolor{color_3rd}{$5.29$} & $58$ & \cellcolor{color_1st}{$4.88$} & $32$ & \cellcolor{color_2nd}{$4.91$} & $3$ & \cellcolor{color_4th}{$5.94$}\\\hline
SNF & $7866$ & $15.07$ & $184$ & \cellcolor{color_2nd}{$2.89$} & $101$ & \cellcolor{color_1st}{$2.85$} & $56$ & \cellcolor{color_3rd}{$2.91$} & $7$ & \cellcolor{color_4th}{$3.79$}\\\Xhline{1pt}
\end{tabular}
\label{tab4}
\end{table*}

This supplemental text material mainly discusses the influence of the max cluster size in the constrained EG clustering to the final rotation averaging results of our proposed method.

We perform our proposed rotation averaging method with $5$ different max cluster sizes, which are $\varGamma=1,50,100,200,\infty$. Here, $\varGamma=1$ means that each camera forms a cluster, \emph{i.e.} the situation of \textbf{without clustering} in the ablation studies of the main text; And, $\varGamma=\infty$ means the EG clustering is not constrained, \emph{i.e.} the situation of \textbf{without constraint} in the ablation studies of the main text. Similar to the main text, the experiments are also performed on the 1DSfM and SNF datasets, and the results are shown in Table \ref{tab4}.

From the Table we can see that: 1)~The number of clusters $|\mathcal{C}|$ is positively correlated to the vertex number $|\mathcal{V}|$, and negatively correlated to the max cluster size $\varGamma$; 2)~Our proposed method overall achieves better performance when $\varGamma$ is set to moderate values, \emph{i.e.} $\varGamma=50,100,200$, than the extreme situations, \emph{i.e.} $\varGamma=1,\infty$, and the variation of $\varGamma$ in a proper range would not much influence the final accuracy. The above observation comes to a conclusion that the specific value of $\varGamma$ is not very important when it is in a proper range, but the involvement of (constrained) EG clustering or not is of much significance, which leads to the parameter setting of $\varGamma$ to $100$ in this letter.

In addition, the situation of $\varGamma=\infty$ achieves best performance on $4$ text data, MDR, MND, GDM, and ROF. As the graph clustering result heavily depends on the graph structure, compared with the unconstrained one, the constrained EG clustering is likely to weaken the inner- or inter-connectivity of the clusters and worsen the rotation averaging results on MDR, MND, GDM, and ROF.

\end{document}
```

ASCII, Line 6, Column 22 | Tab Size: 4 | LaTeX

模板示例

- IEEE Signal Processing Letters (SPL) Manuscript

D:\Papers\personal\submission manuscripts\RANSAC RA\IEEEtran\IEEEtran\final\bib-file.bib - Sublime Text (UNREGISTERED)

File Edit Selection Find View Goto Tools Project Preferences Help

bib-file.bib | Mamuscript.tex | Supplementary.tex

```
@article{Blondel-JSTAT-08,
    year = 2008,
    volume = {2008},
    number = {10},
    pages = {P10008},
    author = {Vincent D Blondel and Jean-Loup Guillaume and Renaud Lambiotte and Etienne Lefebvre},
    title = {Fast unfolding of communities in large networks},
    journal = {Journal of Statistical Mechanics: Theory and Experiment},
}

@INPROCEEDINGS{Chatterjee-ICCV-13,
    author={A. {Chatterjee} and V. M. {Govindu}},
    booktitle={IEEE International Conference on Computer Vision (ICCV)},
    title={Efficient and Robust Large-Scale Rotation Averaging},
    year={2013},
    pages={521-528},
}

@ARTICLE{Chatterjee-TPAMI-18,
    author={A. Chatterjee and V. M. Govindu},
    journal={IEEE Transactions on Pattern Analysis and Machine Intelligence},
    title={Robust Relative Rotation Averaging},
    year={2018},
    volume={40},
    number={4},
    pages={958-972},
}

@ARTICLE{Crandall-TPAMI-13,
    author={D. {Crandall} and A. {Owens} and N. {Snavely} and D. {Huttenlocher}},
    journal={IEEE Transactions on Pattern Analysis and Machine Intelligence},
    title={{SfM with MRFs: Discrete}-Continuous Optimization for Large-Scale Structure from Motion},
    year={2013},
    volume={35},
    number={12},
    pages={2841-2853},
}

@inproceedings{Cui-CVPR-17,
    title={\Protect{HSfM}: Hybrid Structure-from-Motion},
    author={Cui, Hainan and Gao, Xiang and Shen, Shuhan and Hu, Zhanyi},
    booktitle={IEEE Conference on Computer Vision and Pattern Recognition (CVPR)},
    pages={2393-2402},
    year={2017},
}

@INPROCEEDINGS{Cui-ICIP-17,
    author={H. {Cui} and S. {Shen} and X. {Gao} and Z. {Hu}},
    booktitle={IEEE International Conference on Image Processing (ICIP)},
    title={{CSfM: C}ommunity-based structure from motion},
    year={2017},
    pages={4517-4521},
}

@article{Cui-ISPRS-19,
    title = "Efficient and Robust Large-Scale Structure-from-Motion via Track Selection and Camera Prioritization",
    journal = "ISPRS Journal of Photogrammetry and Remote Sensing",
    volume = "156",
    pages = "202-214",
    year = "2019",
    author = "Hainan Cui and Shuhan Shen and Wei Gao and Hongmin Liu and Zhiheng Wang",
}

@INPROCEEDINGS{Cui-ICCV-15,
    author = {Z. Cui and P. Tan},
    booktitle = {IEEE International Conference on Computer Vision (ICCV)},
    title = {Global Structure-from-Motion by Similarity Averaging},
    year = {2015},
    pages = {864-872},
}

@ARTICLE{Dhillon-TPAMI-07,
```

Line 22, Column 49 Tab Size: 4 BibTeX

课程大纲

- LaTeX一览
- LaTeX基础
  - 认识LaTeX
  - 标点与强调
  - 格式控制
  - 字体与颜色
  - 引用与注释
  - 列表
  - 浮动体与图表
  - 西文排版及其他
- LaTeX公式
- LaTeX进阶

认识LaTeX

- 命令与环境
  - LaTeX的**命令**通常是由一个反斜杠加上命令名称以及花括号内的参数构成的：\command{parameters}，比如\documentclass{article}。有的命令不带参数，例如：\TeX TEX
  - 如果有一些选项是备选的，那么通常会在花括号前用方括号标出：\command[options]{parameters}，比如\documentclass[a4paper]{article}
  - 还有一种重要指令叫做**环境**。它被定义于控制命令\begin{environment}和\end{environment}间的内容。比如

```
\begin{document}
...内容...
\end{document}
```

  - 环境如果有备选参数，只需要写在\begin**[]**{parameters}这里就行
  - 环境可以嵌套

认识LaTeX

- 保留字符
  - LaTeX中有许多字符有着特殊的含义，在生成文档时不会直接打印。

    LaTeX中的保留字符有# $ % & ^ _ { } \，它们的作用分别是：
    - #：自定义命令时，用于标明参数序号
    - $：数学环境命令符
    - %：注释符，在其后的该行命令都会视为注释
    - &: 表格环境中的跳列符
    - ^：数学环境中的上标命令符
    - _：数学环境中的下标命令符
    - { }: 花括号用于标记命令的必选参数，或者标记某一部分命令成为一个整体
    - \：反斜杠用于开始各种LaTeX 命令
  - 以上除了反斜杠外，均能用前加反斜杠的形式输出，即你只需要键入：

    \# \$ \% \& \^ _ \{ \} # $ % & ^ _ { }
  - 对于反斜杠的输出，你可以尝试： $\backslash$ \textbackslash \ \

认识LaTeX

- 导言区
  - 任何一份LaTeX 文档都应当包含以下结构：

```
\documentclass[options]{doc-class}
\begin{document}
    ...
\end{document}
```

  - 其中，在语句\begin{document}之前的内容称为**导言区**。导言区可以留空，以可以进行一些文档的准备操作，相当于C语言中的**头文件**包含
  - 在导言区最常见的是宏包的加载工作，形如：\usepackage{package}。宏包是指一系列已经制作好的功能“模块”，在需要使用一些原生LaTeX不带有的功能时，只需要调用这些宏包就可以了

认识LaTeX

- 导言区
  - 文档类\documentclass的参数doc-class和可选选项*options*见下表

doc-class 文档类	
article	- 科学期刊，演示文稿，短报告，邀请函.
proc	- 基于 article 的会议论文集.
report	- 多章节的长报告、博士论文、短篇书.
book	- 书籍.
slides	- 幻灯片，使用了大号 Scans Serif 字体.
options	
字体	- 默认 10pt，可选 11pt 和 12pt.
页面方向	- 默认竖向 portrait，可选横向 landscape.
纸张尺寸	- 默认 letterpaper，可选用 a4paper, b5paper 等.
分栏	- 默认 onecolumn，还有 twocolumn.
双面打印	- 有 oneside/twoside 两个选项，用于排版奇偶页. article/report 默认单面.
章节分页	- 有 openright/openany 两个选项，决定是在奇数页开启新页或是任意页开启新页. 注意 article 是没有 chapter (“章”) 命令的，默认任意页.
公式对齐	- 默认居中，可改为左对齐 fleqn；默认编号居右，可改为左对齐 leqno.
草稿选项	- 默认 final，可改为 draft，使行溢出的部分显示为黑块.

认识LaTeX

- 文件输出
  - LaTeX的输出一般推荐**.pdf**格式，但在**.tex**文档所在的文件夹下可能还会看到下面的其他文件类型
    - **.sty：宏包文件**
    - **.cls：文档类文件**
    - .aux：交叉引用信息存储文件
    - .log：日志文件
    - .toc：目录文件
    - .lof：图形目录
    - .lot：表格目录
    - **.bib：BIBTEX参考文献数据文件**
    - .bbl：BIBTEX生成的参考文献记录
    - **.bst：BIBTEX模板**
    - .blg：BIBTEX日志

认识LaTeX

- 文件输出
  - LaTeX的输出一般推荐**.pdf**格式，但在**.tex**文档所在的文件夹下可能还会看到下面的其他文件类型
    - **.sty：宏包文件**
    - **.cls：文档类文件**
    - .aux：交叉引用信息存储文件
    - .log：日志文件
    - .toc：目录文件
    - .lof：图形目录
    - .lot：表格目录
    - **.bib：BIBTEX参考文献数据文件**
    - .bbl：BIBTEX生成的参考文献记录
    - **.bst：BIBTEX模板**
    - .blg：BIBTEX日志

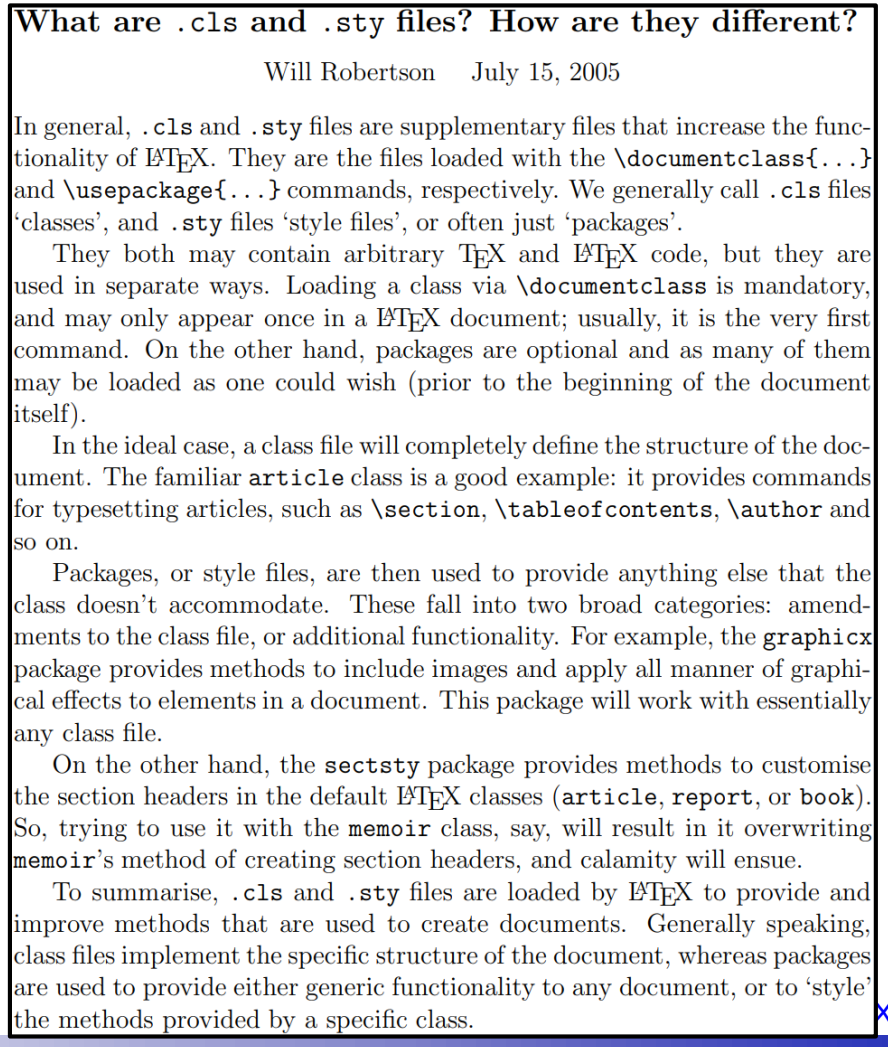

What are .cls and .sty files? How are they different?

Will Robertson July 15, 2005

In general, `.cls` and `.sty` files are supplementary files that increase the functionality of LaTeX. They are the files loaded with the `\documentclass{...}` and `\usepackage{...}` commands, respectively. We generally call `.cls` files 'classes', and `.sty` files 'style files', or often just 'packages'.

They both may contain arbitrary TeX and LaTeX code, but they are used in separate ways. Loading a class via `\documentclass` is mandatory, and may only appear once in a LaTeX document; usually, it is the very first command. On the other hand, packages are optional and as many of them may be loaded as one could wish (prior to the beginning of the document itself).

In the ideal case, a class file will completely define the structure of the document. The familiar `article` class is a good example: it provides commands for typesetting articles, such as `\section`, `\tableofcontents`, `\author` and so on.

Packages, or style files, are then used to provide anything else that the class doesn't accommodate. These fall into two broad categories: amendments to the class file, or additional functionality. For example, the `graphicx` package provides methods to include images and apply all manner of graphical effects to elements in a document. This package will work with essentially any class file.

On the other hand, the `sectsty` package provides methods to customise the section headers in the default LaTeX classes (`article`, `report`, or `book`). So, trying to use it with the `memoir` class, say, will result in it overwriting `memoir`'s method of creating section headers, and calamity will ensue.

To summarise, `.cls` and `.sty` files are loaded by LaTeX to provide and improve methods that are used to create documents. Generally speaking, class files implement the specific structure of the document, whereas packages are used to provide either generic functionality to any document, or to 'style' the methods provided by a specific class.

标点与强调

- 引号
  - LaTeX中左单引号是重音符（`），右单引号是常用的单引号符（'）；左双引号是连续两个重音符（``），右双引号可以是连续两个单引号符（''），也可以是一个双引号符（"）
  - 引号嵌套需要借助\thinspace命令分隔：

```
```Max' is here."\\
``\thinspace`Max' is here."
```

“‘Max’ is here.”

“ ‘Max’ is here.”
```

标点与强调

- 破折、省略号与短横
  - 连字符：输入一个短横“-”，效果如 daughter-in-law
  - 数字起止符：输入两个短横“--”，效果如 page 1–2
  - 破折号：输入三个短横“---”，效果如 Listen—I’m serious
  - 省略号：使用\ldots命令，而非三个句点

```
one, two, three, ..., one hundred.\\
one, two, three, \ldots, one hundred.
```

one, two, three, ..., one hundred.
one, two, three, . . . , one hundred.

标点与强调

- 斜体与粗体
  - 正文斜体命令\emph{text}，正文粗体命令\textbf{text}
  - 公式默认斜体，改正体命令$\mathrm{****}$
  - 公式粗体命令为$\bm{****}$，需要引入宏包\usepackage{bm}

    $z=f(\mathrm{x},\bm{y})$ $z = f(\mathrm{x}, \boldsymbol{y})$

标点与强调

- 下划线与删除线
  - 利用ulem宏包中的命令

```
\uline{下划线} \\
\uuline{双下划线} \\
\dashuline{虚下划线} \\
\dotuline{点下划线} \\
\uwave{波浪线} \\
\sout{删除线} \\
\xout{斜删除线}
```

下划线
双下划线
虚下划线
点下划线
波浪线
删除线
斜删除线

  - 需要注意，ulem宏包重定义了\emph{}命令，使得原来的加斜强调变成了下划线、原来的两次强调就取消强调变成了两次强调就双下划线。通过宏包的normalem选项可以取消这个更改：\usepackage[normalem]{ulem}

格式控制

- 空格、换行与分段
  - 在LaTeX中，多个空格会被视为一个
  - 禁止LaTeX在某个空格处的换行，将空格用~命令替代即可，比如“Fig.~8”
  - 换行：LaTeX会自动转行（**自动断词**）
  - 分段：在每一段的末尾输入两个回车

Pattern design and feature detection. Traditionally, checkerboard [5, 6] and dot [19] patterns have been used for camera calibration. Feature detection in dot patterns is however susceptible to perspective and lens distortion [21]. Recent research includes more robust detectors for checkerboard patterns [11, 24], the use of ridge lines for higher robustness against defocus [10], and calibration with low-rank textures [48]. Ha *et al.* [16] propose the use of triangular patterns, which provide more gradient information for corner refinement than checkerboard patterns. Our proposed calibration pattern similarly increases the available gradients, while however allowing to vary the black/white segment count, enabling us to design better features than [16].

字体与颜色

- 字号
  - 行文会有一个默认的“标准”字号，比如在\documentclass的选项中设置的12pt。LaTeX给出了一系列“相对字号命令”，列出如下表

命令	10pt	11pt	12pt
\tiny	5pt	6pt	6pt
\scriptsize	7pt	8pt	8pt
\footnotesize	8pt	9pt	10pt
\small	9pt	10pt	11pt
\normalsize	10pt	11pt	12pt
\large	12pt	12pt	14pt
\Large	14pt	14pt	17pt
\LARGE	17pt	17pt	20pt
\huge	20pt	20pt	25pt
\Huge	25pt	25pt	25pt

字体与颜色

- 颜色
  - 使用xcolor宏包调用颜色，其具体指令为\textcolor{color-name}{text}
  - xcolor宏包预定义的颜色如下

black	darkgray	lime	pink	violet	blue	gray
magenta	purple	white	brown	green	olive	red
yellow	cyan	lightgray	orange	teal		

  - 可以使用\definecolor{your-color-name}{RGB}{R,G,B}命令自定义颜色
  - 还可以通过“调色”做出新的效果

```
\textcolor{red!70}{百分之70红色}\\
\textcolor{blue!50!black!20!white}
  {50蓝20黑30白}
```

百分之 70 红色
50 蓝 20 黑 30 白

引用与注释

- 标签和引用
  - 使用\label{labelname}命令插入标签（在MS Word 中称为“题注”），然后在其他地方用\ref{labelname}或者\pageref{labelname}命令进行（交叉）引用，分别引用标签的序号与标签所在页的页码
  - 标签一般用于**章节**(section)、**公式**(equation)、**图表**(figure/table)的引用

```
\label{section:this}
\ref{section:this}
\pageref{section:this}
```

- 脚注
  - 使用main text\footnote{footnote text}命令实现

列表

- itemize环境

```
\begin{itemize}
  \item This is the 1st.
  \item[-] And this is the 2nd.
\end{itemize}
```

- This is the 1st.
- And this is the 2nd.

- enumerate环境

```
\begin{enumerate}
  \item First
  \item[Foo] Second
  \item Third
\end{enumerate}
```

1. First

Foo Second

2. Third

- description环境

```
\begin{description}
  \item[LaTeX] Typesetting
    System.
  \item[wkl] A Man.
\end{description}
```

LaTeX Typesetting System.
wkl A Man.

浮动体与图表

- 浮动体
  - 浮动体将**图**或**表**与其**标题**定义为整体，然后动态排版，以解决图、表卡在**换页处**造成的过长的垂直空白的问题
  - 图片的浮动体是**figure**环境，表格的浮动体是**table**环境
  - 一个典型的浮动体例子：

```
\begin{table}[!htb]
    \centering
    \caption{table-cap}
    \label{table-name}
    \begin{tabular}{...}
        ...
    \end{tabular}
\end{table}
```

浮动体与图表

- 浮动体

```
\begin{table}[!htb]
    \centering
    \caption{table-cap}
    \label{table-name}
    \begin{tabular}{...}
        ...
    \end{tabular}
\end{table}
```

  - 浮动体table环境的备选参数!htb含义是：
    - !表示忽略内部参数（比如内部参数对一页中浮动体数量的限制）
    - htb分别表示插入**此处**、插入页面**顶部**、插入页面**底部**，故htb表示优先插入此处，再尝试插入到某页顶，最后尝试插入到页底
    - 此外还有参数p，表示允许为浮动体单独开一页
    - LaTeX的默认参数是tbp
    - 请不要单独使用htbp中的某个参数，以免造成不稳定

浮动体与图表

- 浮动体

```
\begin{table}[!htb]
    \centering
    \caption{table-cap}
    \label{table-name}
    \begin{tabular}{...}
        ...
    \end{tabular}
\end{table}
```

  - \caption{}命令给表格一个标题，写在了表格内容（即tabular环境）之前，表示标题会位于表格上方
  - 对于图片，一般将把此命令写在图片插入命令的下方。注意：\label{}命令请放在caption下方，否则可能出现问题

浮动体与图表

- 图片
  - 图片的插入使用graphicx宏包和\includegraphics[]{}命令

```
\begin{center}
    \includegraphics[width=0.8\linewidth]{ThisPic}
\end{center}
```

  - 可选参数指定了图片宽度为0.8倍该行文字宽。类似地可以指定height（图片高），scale（图片缩放倍数），angle（图片逆时针旋转角度）等
  - 对于Thispic这个参数的写法，LaTeX支持**.pdf**，.eps，.png，.jpg图片扩展名。可以书写带扩展名的图片名称ThisPic.png，也可以不带扩展名。如果不给出扩展名，将按上述四个扩展名的顺序依次搜索文件

浮动体与图表

- 矢量图
  - 矢量图（vector graphics, .SVG .PDF） *vs.* 栅格图（raster graphics, .JPEG .PNG）
  - 定义在二维点上，通过**直线**或**基于数学方程的曲线**连接起来，组合成多边形或其他形状来表示的图形
  - 体积较小，缩放不变

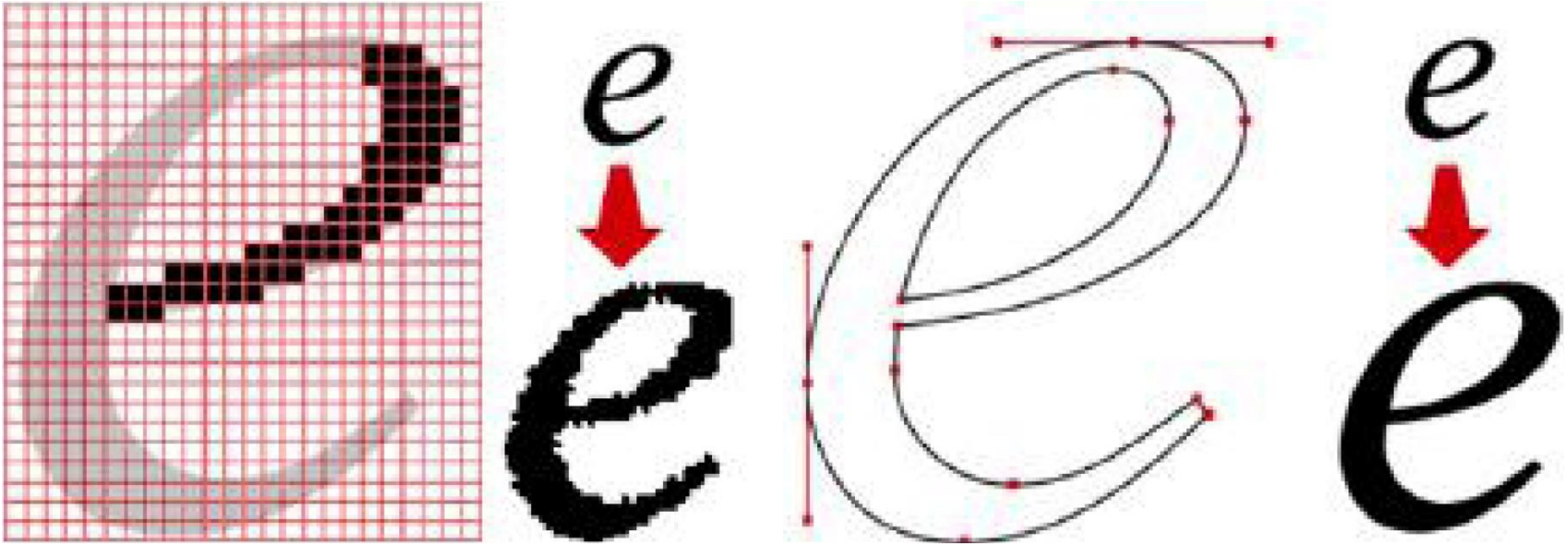

浮动体与图表

- 矢量图
  - **示意图：MS Word**
  - 流程图：MS Visio
  - 数据分析图：MATLAB, Python Matplotlib
  - 处理工具：Adobe Acrobat Pro

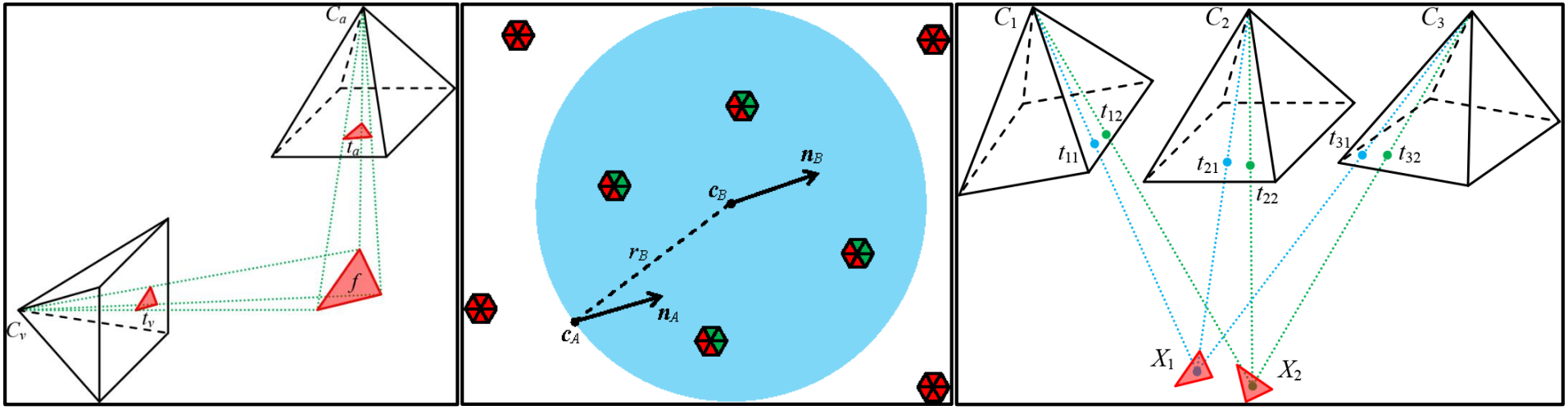

浮动体与图表

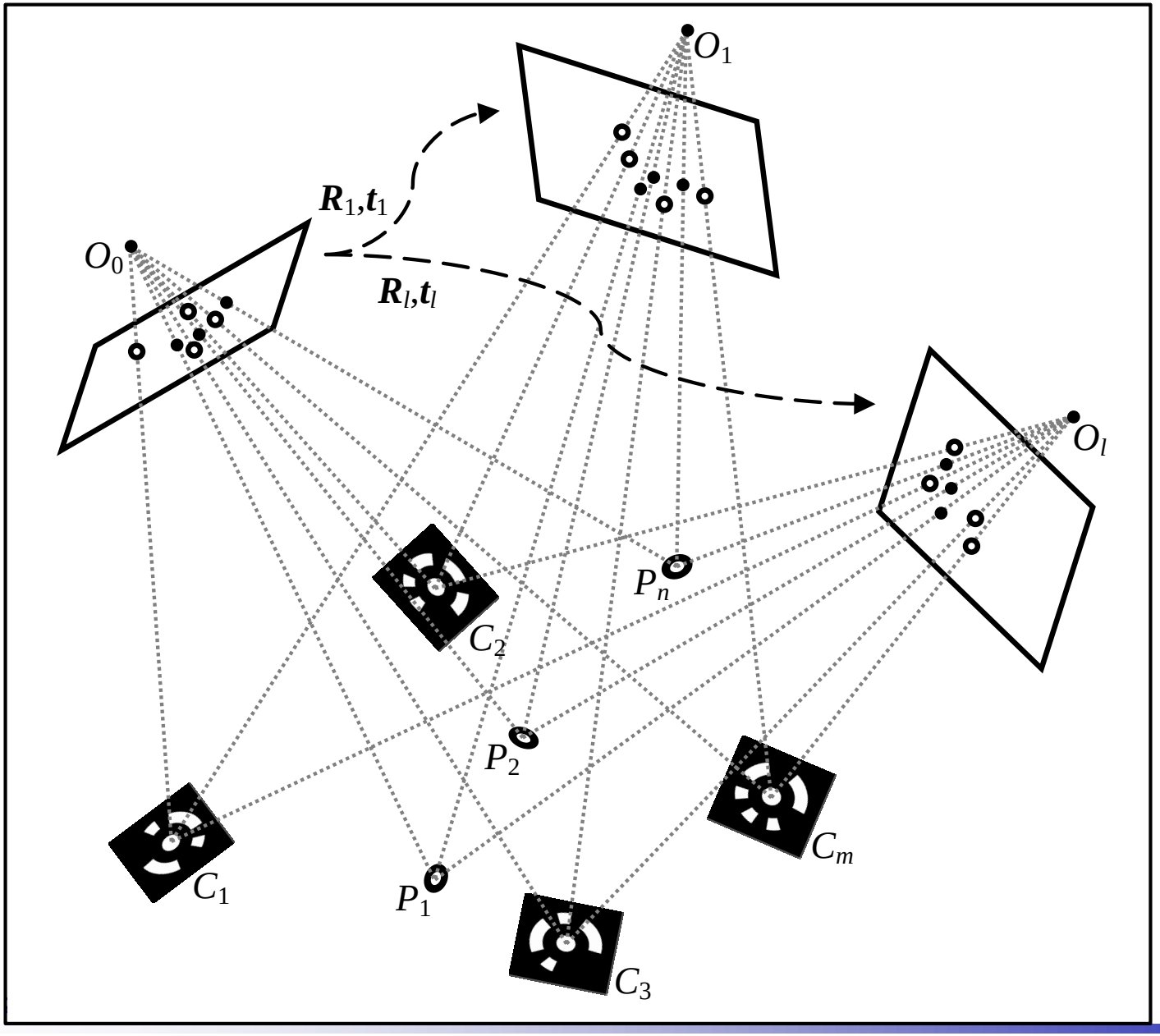
O_1
$\boldsymbol{R}_1,\boldsymbol{t}_1$
O_0
$\boldsymbol{R}_l,\boldsymbol{t}_l$
O_l
P_n
C_2
P_2
C_m
C_1
P_1
C_3

浮动体与图表

- 矢量图
  - 示意图：MS Word
  - **流程图：MS Visio**
  - 数据分析图：MATLAB, Python Matplotlib
  - 处理工具：Adobe Acrobat Pro

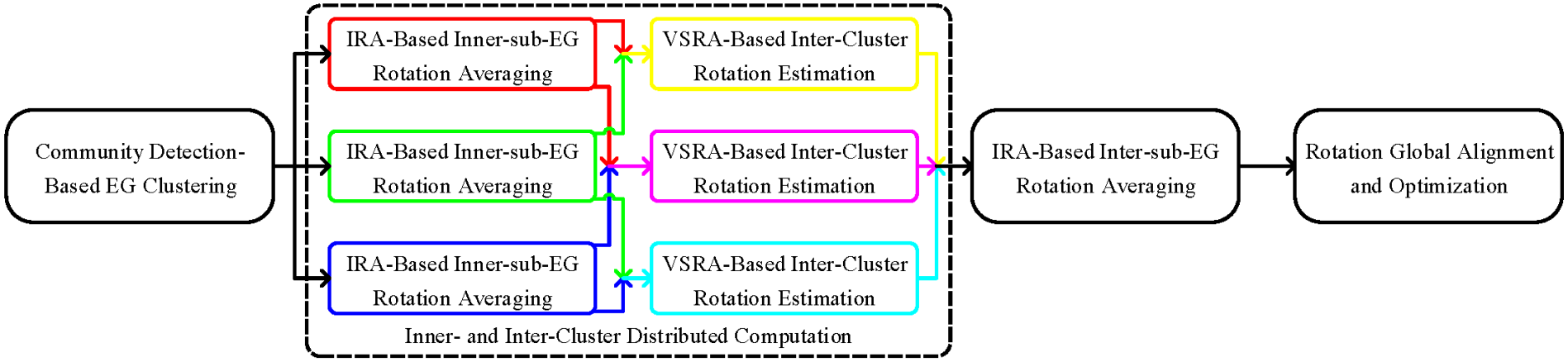

浮动体与图表

- 矢量图

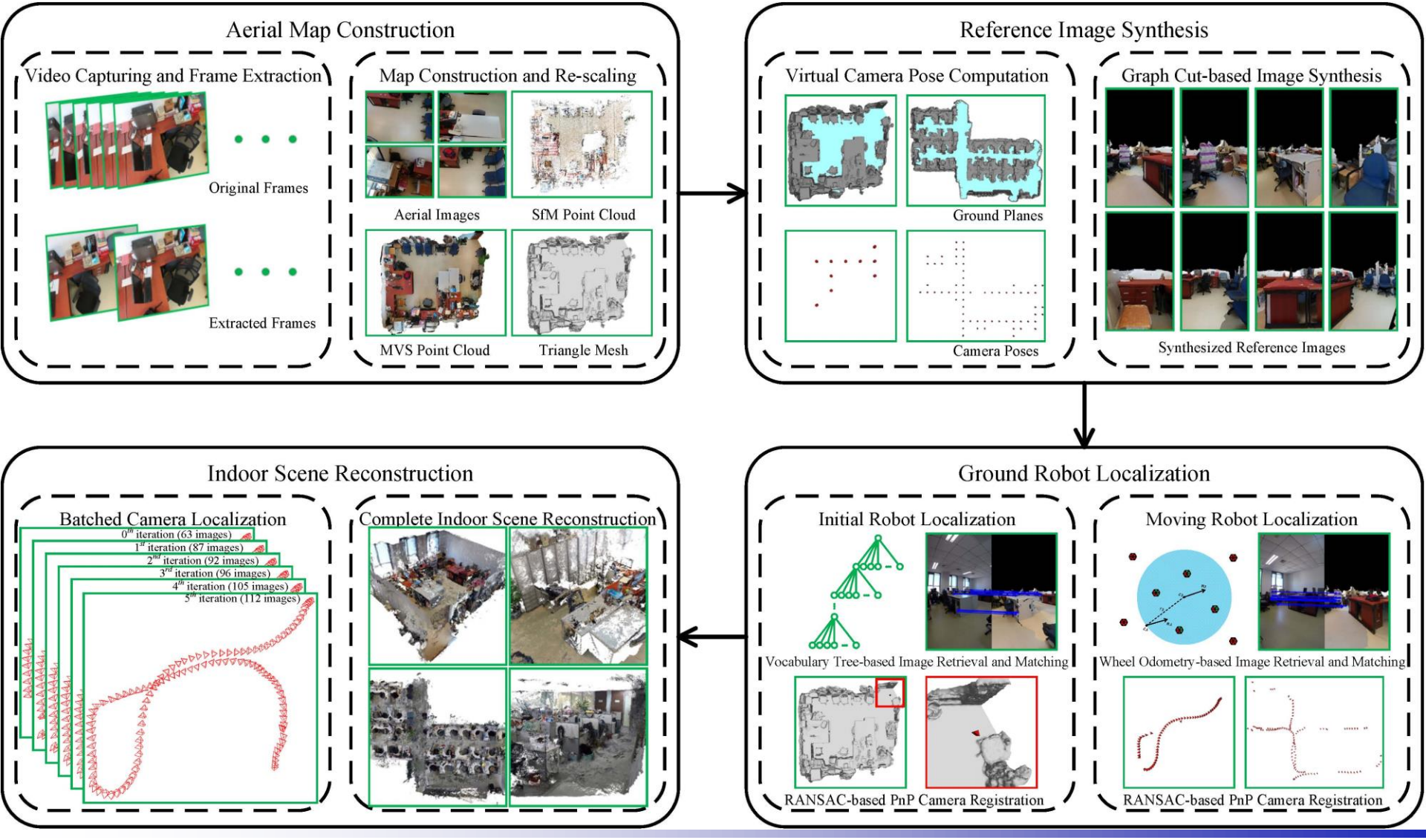
Aerial Map Construction
Video Capturing and Frame Extraction
Original Frames
Extracted Frames
Map Construction and Re-scaling
Aerial Images
SfM Point Cloud
MVS Point Cloud
Triangle Mesh
Reference Image Synthesis
Virtual Camera Pose Computation
Ground Planes
Camera Poses
Graph Cut-based Image Synthesis
Synthesized Reference Images
Indoor Scene Reconstruction
Batched Camera Localization
0th iteration (63 images)
1st iteration (87 images)
2nd iteration (92 images)
3rd iteration (96 images)
4th iteration (105 images)
5th iteration (112 images)
Complete Indoor Scene Reconstruction
Ground Robot Localization
Initial Robot Localization
Vocabulary Tree-based Image Retrieval and Matching
RANSAC-based PnP Camera Registration
Moving Robot Localization
Wheel Odometry-based Image Retrieval and Matching
RANSAC-based PnP Camera Registration

浮动体与图表

- 矢量图
  - 示意图：MS Word
  - 流程图：MS Visio
  - **数据分析图：MATLAB, Python Matplotlib**
  - 处理工具：Adobe Acrobat Pro

```
1   x=1:1:5;
2   a=[203.024,113.857,256.259,244.888,293.376];
3   b=[334.4,143.2,297.4,487.2,596.2];
4   plot(x,a,'-*b',x,b,'-or');
5   axis([0,6,0,700]);
6   set(gca,'XTick',[0:1:6]);
7   set(gca,'YTick',[0:100:700]);
8   legend('Neo4j','MongoDB');
9   xlabel('深度');
10  ylabel('时间（ms）');
```

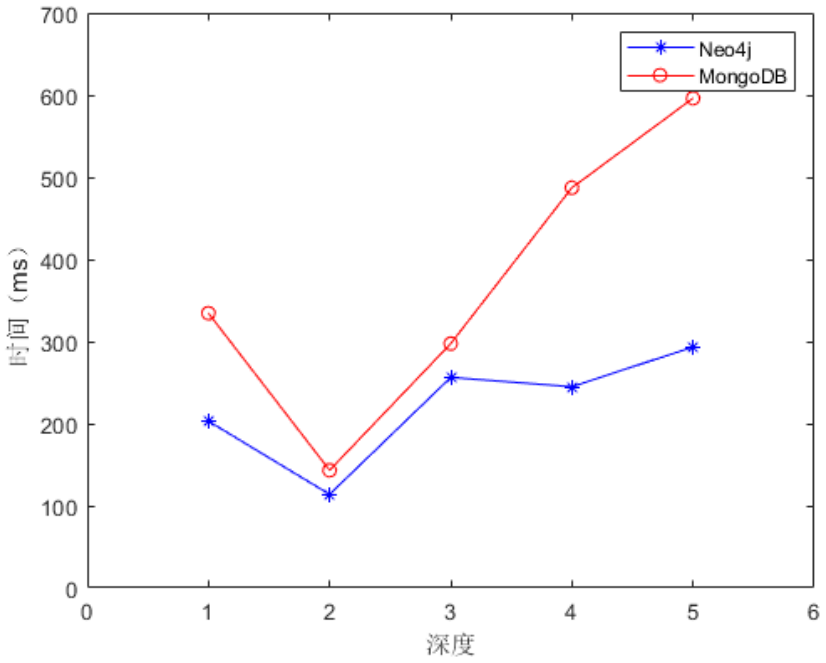

浮动体与图表

- 矢量图
  - 示意图：MS Word
  - 流程图：MS Visio
  - **数据分析图：MATLAB, Python Matplotlib**
  - 处理工具：Adobe Acrobat Pro

```
In [1]: import matplotlib.pyplot as plt
In [2]: x_data = ['2011','2012','2013','2014','2015','2016','2017']
In [3]: y_data = [58000,60200,63000,71000,84000,90500,107000]
In [4]: plt.plot(x_data,y_data)
```

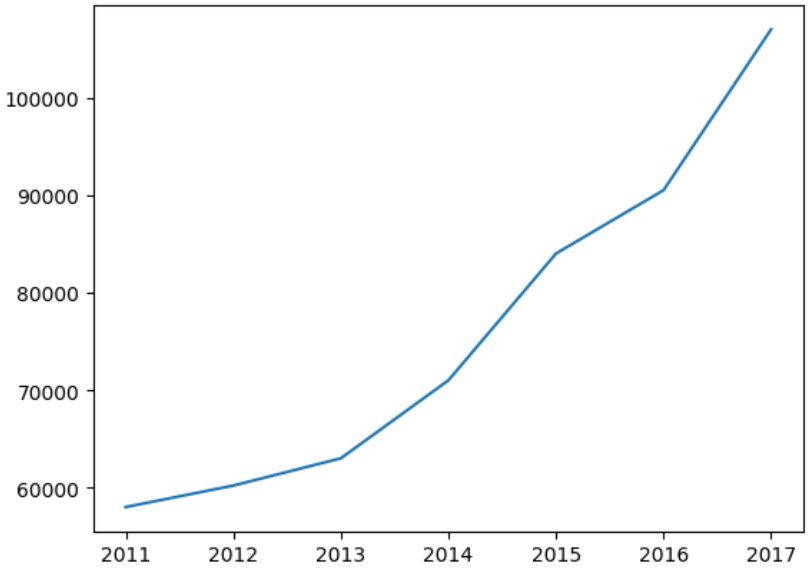

浮动体与图表

- 矢量图
  - 示意图：MS Word
  - 流程图：MS Visio
  - 数据分析图：MATLAB, Python Matplotlib
  - **处理工具：Adobe Acrobat Pro**
    - 另存为.PDF格式并进行**页面剪裁**

浮动体与图表

- 表格
  - LaTeX原生的表格功能非常有限，甚至不支持单元格跨行和表格跨页

```
\begin{center}
  \begin{tabular}[c]{|l|c||p{3em}
    r@{-}} \hline\hline
    A & B & C & d\\D & E & F &
    g\\
    \cline{1-2}
    \multicolumn{2}{|c|}{G}&H&i\\
    \hline
  \end{tabular}
\end{center}
```

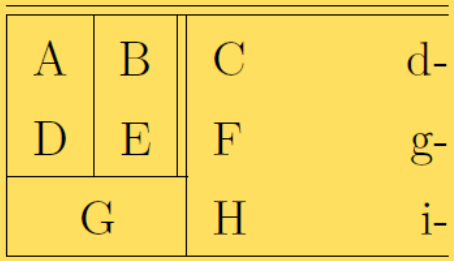

浮动体与图表

- 表格

```
\begin{center}
  \begin{tabular}[c]{|l|c||p{3em}
    r@{-}} \hline\hline
    A & B & C & d\\D & E & F &
    g\\
    \cline{1-2}
    \multicolumn{2}{|c|}{G}&H&i\\
    \hline
  \end{tabular}
\end{center}
```

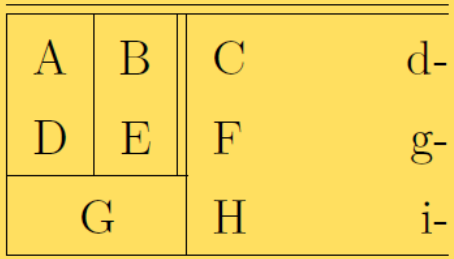

- 参数说明
  - 可选参数**对齐方式**：[t]表示表格上端与所在行的网格线对齐。如果与它同一行的有文字的话，文字是与表格上端同高的。参数[b]与参数[c]分别表示下端同高与中央同高。t=top, b=bottom, c=center

浮动体与图表

- 表格

```
\begin{center}
  \begin{tabular}[c]{|l|c||p{3em}
    r@{-}} \hline\hline
    A & B & C & d\\D & E & F &
    g\\
    \cline{1-2}
    \multicolumn{2}{|c|}{G}&H&i\\
    \hline
  \end{tabular}
\end{center}
```

A	B	C	d-
D	E	F	g-
G		H	i-

- 参数说明
  - 必选参数**列格式**：竖线符号“|”来表示竖直表线，连续两个竖线符号“||”表示双竖直表线。最右边留空了，表示没有竖直表线。或者可以使用“@{}”表示没有竖直表线，也可以用“@{-}”这样的形式把竖直表线替换成“-”。此处的l, c, r分别表示从左往右三列分别左对齐、居中对齐、右对齐文字。在使用l, c, r时，表格宽度会自动调整，也可以用”p{3em}”这样的命指定某一列的宽度

浮动体与图表

- 表格

```
\begin{center}
  \begin{tabular}[c]{|l|c||p{3em}
    r@{-}} \hline\hline
    A & B & C & d\\D & E & F &
    g\\
    \cline{1-2}
    \multicolumn{2}{|c|}{G}&H&i\\
    \hline
  \end{tabular}
\end{center}
```

A	B	C	d-
D	E	F	g-
G		H	i-

- 参数说明
  - 在tabular环境内部，命令\hline来绘制水平表线。命令\cline{i-j}用于绘制横跨从i到j行的水平表线，两个连续的\hline命令可以画双线
  - 在tabular环境内部，命令“**&**”用于把光标跳入该行下一列的单元格，每行最后使用两个反斜杠命令“****”跳入下一行

浮动体与图表

- 表格
  - multirow宏包

```latex
% \usepackage{multirow}
\begin{center}
\begin{tabular}{|c|c|c|}
  \hline
  \multirow{2}{2cm}{A Text!}
    & ABC & DEF \\
  \cline{2-3} & abc & def \\
  \hline
  \multicolumn{2}{|c|}
    {\multirow{2}*{Nothing}} &
    XYZ \\
  \multicolumn{2}{|c|}{} & xyz \\
  \hline
\end{tabular}
\end{center}
```

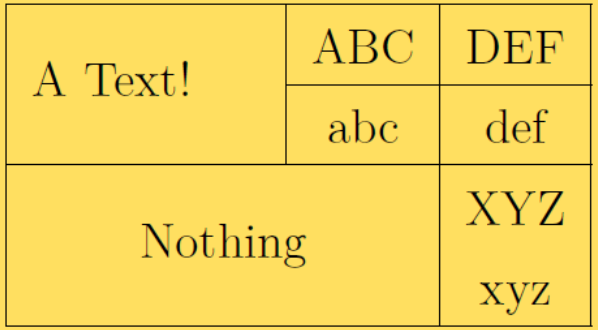

浮动体与图表

- 表格
  - multirow宏包

```
% \usepackage{multirow}
\begin{center}
\begin{tabular}{|c|c|c|}
  \hline
  \multirow{2}{2cm}{A Text!}
    & ABC & DEF \\
  \cline{2-3} & abc & def \\
  \hline
  \multicolumn{2}{|c|}
    {\multirow{2}*{Nothing}} &
    XYZ \\
  \multicolumn{2}{|c|}{} & xyz \\
  \hline
\end{tabular}
```

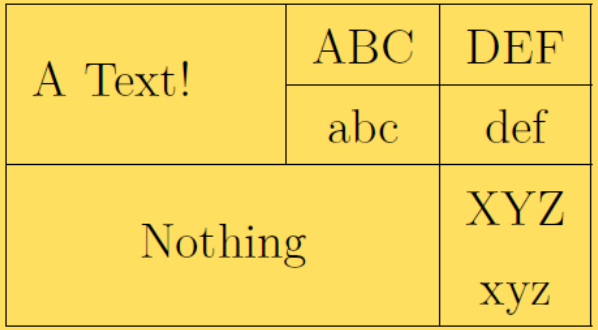

  - 如果同时跨行跨列，必须把\multirow命令放在\multicolumn内部
  - 用\multirow和\multicolumn作用于单独的1行或1列，能临时改变某单元格的**对齐方式**。如果用星号*代替列样式，表示自适应宽度

浮动体与图表

- 表格
  - makecell宏包

```
\begin{tabular}{ccc}
\Xhline{2pt}
\multirow{2}*{X} &
\multicolumn{2}{c}{Hey}\\
\Xcline{2-3}{0.4pt}
& Left & Right \\
\Xhline{1pt}
a & A & B \\
b & C & D \\
\Xhline{2pt}
\end{tabular}
```

X	Hey	
	Left	Right
a	A	B
b	C	D

    - 该宏包提供了\Xhline和\Xcline命令，可指定横线的线宽以模仿三线表

浮动体与图表

- 表格
  - diagbox宏包

```
\begin{tabular}{c|cc}
\diagbox{左边}{中间}{右边} & A &
    B \\
\hline
1 & A1 & B1 \\
2 & A2 & B2
\end{tabular}
```

中间 \ 右边 / 左边	A	B
1	A1	B1
2	A2	B2

浮动体与图表

- 表格排版练习

```
\begin{table}[!htb]
    \centering
    \caption{table-cap}
    \label{table-name}
    \begin{tabular}{...}
        ...
    \end{tabular}
\end{table}
```

```
\begin{tabular}{ccc}
\Xhline{2pt}
\multirow{2}*{X} &
\multicolumn{2}{c}{Hey}\\
\Xcline{2-3}{0.4pt}
& Left & Right \\
\Xhline{1pt}
a & A & B \\
b & C & D \\
\Xhline{2pt}
\end{tabular}
```

X	Hey	
	Left	Right
a	A	B
b	C	D

浮动体与图表

- 表格排版练习

	CD	ECD	LFD	#V	#F
Atlas0	1.487	1.866	3644.91	7446	14888
Atlas25	**1.170**	2.069	3436.14	2500	4050
OccNet_{32}	2.538	6.245	3795.23	1511	3017
OccNet_{64}	1.950	6.654	3254.55	6756	13508
OccNet_{128}	1.945	6.766	3224.33	27270	54538
IM-NET_{32}	2.361	4.617	3700.22	1204	2404
IM-NET_{64}	1.467	4.426	2940.56	5007	10009
IM-NET_{128}	1.387	1.971	2810.47	20504	41005
IM-NET_{256}	1.371	2.273	**2804.77**	82965	165929
Ours	1.432	**0.743**	2939.15	**1191**	**1913**

浮动体与图表

- 表格排版练习

Method	DA		DC		CD	
	Mean	Var.	Mean	Var.	Mean	RMS
PSR(trim 8)	0.473	1.33	0.327	0.220	3.16	12.5
PSR(trim 9.5)	0.330	0.441	0.345	0.438	**1.17**	4.49
Ours	**0.321**	**0.285**	**0.304**	**0.0888**	1.46	**4.42**

An Invitation to LaTeX

Xiang Gao, Lecturer

E-mail: xgao@ouc.edu.cn | Web: https://ouc-xgao.github.io/

College of Engineering, Ocean University of China

课程回顾

- LaTeX一览
  - LaTeX简介
    - What?，Why?，How?，(Negligible) drawbacks，Hello world!
  - 课程简介
    - 课程目标，参考书目
  - 模板示例
    - IEEE Trans.，Springer IJCV，IEEE CVPR，ACM SIGGRAPH，IEEE SPL
- LaTeX基础
  - 认识LaTeX
    - 命令与环境，保留字符，导言区，文件输出
  - 标点与强调
    - 引号，破折、省略号与短横，斜体与粗体，下划线与删除线

课程回顾

- LaTeX基础（续）
  - 格式控制
    - 空格、换行与分段
  - 字体与颜色
    - 字号，颜色
  - 引用与注释
    - **标签与引用**，脚注
  - 列表
    - itemize、enumerate、description环境
  - **浮动体与图表**
    - 浮动体，图片，矢量图，表格

西文排版及其他

- 连写
  - LaTeX排版中，如果输入ff, fl, fi, ffi等内容，它们默认会连写 ff, fl, fi, ffi
  - 在字母中间插入“{}”以强制不连写：

```
It's difficult to find \ldots\\
It's dif{}f{}icult to f{}ind \ldots
```

It's difficult to find ...
It's difficult to find ...

- 断词
  - 行末的英文单词太长，LaTeX就自动会以其音节断词。如果想指定某些单词的断词位置，使用断词命令\hyphenation{}

```
1 \hyphenation{Hy-phen-a-tion FORTRAN}
```

  - 这个例子**允许**Hyphenation，hyphenation在连字符处断词，同时**禁止**FORTRAN, Fortran, fortran断词

课程大纲

- LaTeX一览
- LaTeX基础
- LaTeX公式
  - 行内与行间公式
  - 基本命令
  - 数学符号与字体
  - 公式截图识别
  - 公式排版练习
- LaTeX进阶

行内与行间公式

- 行内公式
  - 将公式嵌入到文段的排版方式，主要要求公式垂直距离不能过高，否则影响排版效果，行内公式的书写方式：

```
$...$ 或者 \(...\) 或者 \begin{math}...\end{math}
```

  - 一般推荐第一或第二种方式。例：$\sum_{i=1}^{n}a_i$ $\sum_{i=1}^{n} a_i$

行间与行内公式

- 行间公式
  - 行间公式也称行外公式，书写方式：

```
\[...\] 或者 \begin{displaymath}...\end{displaymath}
或者 amsmath 提供的 \begin{equation*}...\end{equation*}
```

  - 一般也推荐第一种命令，例：\[\sum_{i=1}^n{a_i}\] $$\sum_{i=1}^{n} a_i$$
  - 可以看出，即使输出相同的内容，行内和行间的排版也是有区别的，比如累加符号的上下标位置
  - 如果行间公式需要编号，使用equation环境，还可以插入标签

```
\begin{equation}
\label{eq:NoExample}
  |\epsilon|>M
\end{equation}
```

$$|\epsilon| > M \tag{4.1}$$

基本命令

- 上下标与虚位
  - 用低划线“_”和尖角符“^”表示上标和下标

```
$a^3_{ij}$ \\
${a_{ij}}^3\text{或}a_{ij}{}^3$\\
$\mathrm{e}^{x^2}\geq 1$
```

a_{ij}^3
${a_{ij}}^3$或$a_{ij}{}^3$
$\mathrm{e}^{x^2}\geq 1$

  - 此外，被称为虚位命令，其作用可由下例体会：

```
${}^{12}_{6}\mathrm{C}$ \\
${}^{12}_{\phantom{1}6}
\mathrm{C}$ \\
$a^3_{ij}$ \\
$a^{\phantom{ij}3}_{ij}$
```

${}^{12}_{6}\mathrm{C}$
${}^{12}_{6}\mathrm{C}$
a^3_{ij}
a^{3}_{ij}

基本命令

- 分式、根式与堆叠
  - 分式使用\frac{a}{b}命令。或者使用amsmath宏包支持的\dfrac{a}{b}、\tfrac{a}{b}命令来强制获得行间公式、行内公式大小的分数

```
\[\frac{x}{y}+\dfrac{x}{y}
+\tfrac{a}{b}\]
```

$$\frac{x}{y}+\dfrac{x}{y}+\tfrac{a}{b}$$

  - 空根式用\surd输出，更常用的是\sqrt[]{}

```
$\sqrt{2} \qquad \surd$\\
$\sqrt[\beta]{k}$
```

$\sqrt{2} \qquad \surd$
$\sqrt[\beta]{k}$

基本命令

- 分式、根式与堆叠
  - 划线命令使用\underline{}和\overline{}
  - 水平括号使用brace“{”或者bracket“[”代替line，例如\underbrace{}

```
$\overline{m+n}$ \\
$\underbrace{a_1+\ldots+a_n}_{n}$
$\overbrace{a_1+\ldots+a_n}^{n}$
% 可选参数：线宽；竖直空距
$\underbracket[0.4pt][1ex]
  {a_1+\cdots+a_n}_n$
```

$$\overline{m+n}$$

$$\underbrace{a_1+\ldots+a_n}_{n} \qquad \overbrace{a_1+\ldots+a_n}^{n}$$

$$\underbracket[0.4pt][1ex]{a_1+\cdots+a_n}_{n}$$

  - 利用\overrightarrow{}与\overleftarrow{}命令输出能堆叠到其他对象上的箭头符，比如向量符号

```
$\vec
  a\quad\overrightarrow{PQ}$
$\overleftarrow{EF}$
```

$$\vec{a} \quad \overrightarrow{PQ} \; \overleftarrow{EF}$$

基本命令

- 分式、根式与堆叠
  - 利用\xrightarrow{}与\xleftarrow{}命令输出能够添加上下堆叠的箭头符

```
\[ a\xleftarrow{x+y+z} b \]
\[ c\xrightarrow[x<y]{a*b*c}d \]
```

$$a \xleftarrow{x+y+z} b$$

$$c \xrightarrow[x<y]{a*b*c} d$$

  - 尖帽符号、波浪符号，还有yhmath宏包支持的圆弧符号

```
$\hat{A}\quad\widehat{AB}$\\
$\tilde{C}\quad\widetilde{CD}$
\qquad\wideparen{APB}$
```

$$\hat{A} \quad \widehat{AB}$$
$$\tilde{C} \quad \widetilde{CD} \qquad \overparen{APB}$$

  - 强制堆叠命令\stackrel{}, \overset{}, underset{}
  - 被强制堆叠的符号与上标同等大小

```
$\int f(x) \stackrel{?}{=} 1$\\
$A\overset{abc}{=}B$ \quad
    $C\underset{def}{=}D$
```

$$\int f(x) \stackrel{?}{=} 1$$
$$A \overset{abc}{=} B \quad C \underset{def}{=} D$$

基本命令

- 累加与累积
  - 使用\sum_{}^{}和\prod_{}^{}命令，效果如下：

```
\[\sum_{i=1}^{n}a_i=1 \qquad
\prod_{j=1}^{n}b_j=1\]
```

$$\sum_{i=1}^{n} a_i = 1 \qquad \prod_{j=1}^{n} b_j = 1$$

  - 有时需要复杂的堆叠方式，效果如下：

```
\[\sum_{\substack{0<i<n \\
  0<j<m}} p_{ij}=
  \prod_{\begin{subarray}{l}
  i\in I \\  1<j<m
  \end{subarray}}q_{ij}\]
```

$$\sum_{\substack{0<i<n \\ 0<j<m}} p_{ij} = \prod_{\substack{i\in I \\ 1<j<m}} q_{ij}$$

基本命令

- 矩阵与省略号
  - 矩阵的排版可以通过array环境和自适应定界符“\left”, “\right”完成：

```
\[\mathbf{A}=
\left(\begin{array}{ccc}
x_{11} & x_{12} & \ldots \\
x_{21} & x_{22} & \ldots \\
\vdots & \vdots & \ddots
\end{array}\right)\]
```

$$\mathbf{A}=\left(\begin{array}{ccc} x_{11} & x_{12} & \ldots \\ x_{21} & x_{22} & \ldots \\ \vdots & \vdots & \ddots \end{array}\right)$$

  - 宏包amsmath还支持行内小矩阵\smallmatrix：

```
矩阵 $\left(\begin{smallmatrix}
x & -y\\ y & x\end{smallmatrix}
\right)$ 可以显示在行内.
```

矩阵 $\left(\begin{smallmatrix} x & -y \\ y & x \end{smallmatrix}\right)$ 可以显示在行内.

基本命令

- 分段函数与联立方程
  - 用cases环境书写分段函数，它自动生成一个比\left{更紧凑的花括号

```
\[ |x| = \left\{
\begin{array}{rl}
-x & \text{if } x < 0,\\
0 & \text{if } x = 0,\\
x & \text{if } x > 0.
\end{array} \right. \]
```

$$|x| = \begin{cases} -x & \text{if } x < 0, \\ 0 & \text{if } x = 0, \\ x & \text{if } x > 0. \end{cases}$$

```
\[ |x| =
\begin{cases}
-x & \text{if } x < 0,\\
0 & \text{if } x = 0,\\
x & \text{if } x > 0.
\end{cases} \]
```

$$|x| = \begin{cases} -x & \text{if } x < 0, \\ 0 & \text{if } x = 0, \\ x & \text{if } x > 0. \end{cases}$$

基本命令

- 多行公式及其编号
  - 多行公式可以使用amsmath下的align环境
  - 这个环境会自动对齐等号或者不等号，所以必要时用“&”指定对齐位置

```
\begin{align}
  a^2  &= a\cdot a \\
       &= a*a      \\
       &= a^2
\end{align}
```

$$
\begin{aligned}
a^2 &= a \cdot a && (4.2)\\
&= a * a && (4.3)\\
&= a^2 && (4.4)
\end{aligned}
$$

  - LaTeX中长公式不能自动换行，可如上自行指定**断行**与**对齐**位置
  - align 环境会给每行公式都编号，可以用\notag去掉某行的编号

```
\begin{align}
a^2 &= a\cdot a \\
&= a*a \notag \\
&= a^2
\end{align}
```

$$
\begin{aligned}
a^2 &= a \cdot a && (1)\\
&= a * a \\
&= a^2 && (2)
\end{aligned}
$$

基本命令

- 多行公式及其编号
  - align还能够对齐多组公式，除等号前的&之外，公式之间也用&分隔：

```
\begin{align}
a &=1   &   b &=2    & c &=3    \\
d &=-1 &   e &=-2   & f &=-5
\end{align}
```

$$a = 1 \qquad b = 2 \qquad c = 3 \tag{4.8}$$
$$d = -1 \qquad e = -2 \qquad f = -5 \tag{4.9}$$

  - 另一常见需求是将多个公式组在一起公用一个编号，编号位于公式的居中位置，为此，amsmath宏包提供了aligned环境，与equation 环境套用

```
\begin{equation}
\begin{aligned}
a &= b + c \\
d &= e + f + g \\
h + i &= j + k \\
l + m &= n
\end{aligned}
\end{equation}
```

$$\begin{aligned} a &= b + c \\ d &= e + f + g \\ h + i &= j + k \\ l + m &= n \end{aligned} \tag{4.13}$$

数学符号与字体

- 字体

原生数学字体表

\mathrm{ABCDabcde 1234}	ABCDabcde1234
\mathit{ABCDabcde 1234}	*ABCDabcde123*
\mathnormal{ABCDabcde 1234}	*ABCDabcde*1234
\mathcal{ABCDabcde 1234}	$\mathcal{ABCD}\dashv\vert\vert\lceil\rceil\infty\in\ni\triangle$

宏包数学字体表

\mathscr{ABCDabcde 1234}	mathrsfs
$\mathscr{A}\,\mathscr{B}\mathscr{C}\,\mathscr{D}$	
\mathfrak{ABCDabcde 1234}	amsfonts 或者 amssymb
$\mathfrak{ABCD}$abcde1234	
\mathbb{ABCDabcde 1234}	amsfonts 或者 amssymb
$\mathbb{ABCD}\beth\nvDash\nvdash\not\supset$	

数学符号与字体

- 字号

数学符号尺寸

命令	尺寸	示例
\displaystyle	行间公式尺寸	$\sum a$
\textstyle	行内公式尺寸	$\sum a$
\scriptstyle	上下标尺寸	a
\scriptscriptstyle	次级上下标尺寸	a

```
\[
r = \frac
  {\sum_{i=1}^n (x_i- x)(y_i- y)}
  {\displaystyle \left[
    \sum_{i=1}^n (x_i-x)^2
    \sum_{i=1}^n (y_i-y)^2
  \right]^{1/2} }
\]
```

$$r = \frac{\sum_{i=1}^{n}(x_i - x)(y_i - y)}{\displaystyle\left[\sum_{i=1}^{n}(x_i - x)^2 \sum_{i=1}^{n}(y_i - y)^2\right]^{1/2}}$$

数学符号与字体

- 定界符

定界符

(	(	[	[or \lbrack	↑	\uparrow
)	)	]	] or \rbrack	↓	\downarrow
{	{ or \lbrace	}	} or \rbrace	↕	\updownarrow
⟨	\langle	⟩	\rangle	\	\backslash
⌊	\lfloor	⌋	\rfloor	⇕	\Updownarrow
⌈	\lceil	⌉	\rceil	⇑	\Uparrow
‖	\\| or \Vert	|	| or \vert	⇓	\Downarrow

– 以下需要 amssymb 宏包 –

⌜	\ulcorner	⌝	\urcorner
⌞	\llcorner	⌟	\lrcorner

数学符号与字体

- 定界符
  - 使用\left, \right还有\middle能够使定界符自适应式子的高度:

```
\[P\left(X \middle\vert
    Y=0\right)
=\left.\int_0^1 p(t)\ud
    t\middle/ N\right.\]
```

$$P\left(X \middle\vert Y=0\right) =\left.\int_0^1 p(t)\ud t\middle/ N\right.$$

  - 通过如下命令可以手动指定定界符尺寸:

```
% 加l, r, m对应上述三种自适应命令
$(\big(\Big(\bigg(\Bigg<\qquad
\bigl[\frac{x+y}{x^2}\bigr]$
```

$$(\big(\Big(\bigg(\Bigg\langle \qquad \bigl[\frac{x+y}{x^2}\bigr]$$

数学符号与字体

- 希腊字母

希腊字母表

α	\alpha	θ	\theta	o	o	υ	\upsilon
β	\beta	ϑ	\vartheta	π	\pi	ϕ	\phi
γ	\gamma	ι	\iota	ϖ	\varpi	φ	\varphi
δ	\delta	κ	\kappa	ρ	\rho	χ	\chi
ϵ	\epsilon	λ	\lambda	ϱ	\varrho	ψ	\psi
ε	\varepsilon	μ	\mu	σ	\sigma	ω	\omega
ζ	\zeta	ν	\nu	ς	\varsigma	η	\eta
ξ	\xi	τ	\tau				
A	A	B	B	Γ	\Gamma	$\varGamma$	\varGamma
Δ	\Delta	$\varDelta$	\varDelta	E	E	Z	Z
H	H	Θ	\Theta	$\varTheta$	\varTheta	I	I
Λ	\Lambda	$\varLambda$	\varLambda	M	M	N	N
Ξ	\Xi	$\varXi$	\varXi	O	O	Π	\Pi
$\varPi$	\varPi	P	P	Σ	\Sigma	$\varSigma$	\varSigma
T	T	Υ	\Upsilon	$\varUpsilon$	\varUpsilon	Φ	\Phi
$\varPhi$	\varPhi	X	X	Ψ	\Psi	$\varPsi$	\varPsi
Ω	\Omega	$\varOmega$	\varOmega				

数学符号与字体

- 二元运算符

二元运算符

$+$	+	$-$	-	$\times$	\times	$\div$	\div
$\pm$	\pm	$\mp$	\mp	$\circ$	\circ	$\triangleright$	\triangleright
$\cdot$	\cdot	$\star$	\star	$*$	\ast	$\triangleleft$	\triangleleft
$\cup$	\cup	$\cap$	\cap	$\setminus$	\setminus	$\bullet$	\bullet
$\oplus$	\oplus	$\ominus$	\ominus	$\otimes$	\otimes	$\oslash$	\oslash
$\odot$	\odot	$\bigcirc$	\bigcirc	$\vee$	\vee,\lor	$\wedge$	\wedge,\land
$\bigcup$	\bigcup	$\bigcap$	\bigcap	$\bigvee$	\bigvee	$\bigwedge$	\bigwedge

数学符号与字体

- 二元关系符

二元关系符

$<$	<	$>$	>	$\leq$	\le(q)	$\geq$	\ge(q)
$\ll$	\ll	$\gg$	\gg	$\equiv$	\equiv	$\neq$	\neq
$\prec$	\prec	$\succ$	\succ	$\preceq$	\preceq	$\succeq$	\succeq
$\sim$	\sim	$\simeq$	\simeq	$\cong$	\cong	$\approx$	\approx
$\subset$	\subset	$\supset$	\supset	$\subseteq$	\subseteq	$\supseteq$	\supseteq
$\in$	\in	$\ni$	\ni	$\notin$	\notin	$\propto$	\propto
$\parallel$	\parallel	$\perp$	\perp	$\smile$	\smile	$\frown$	\frown
$\asymp$	\asymp	$\bowtie$	\bowtie	$\vdash$	\vdash	$\dashv$	\dashv

amssymb 二元关系符

$\leqslant$	\leqslant	$\geqslant$	\geqslant	$\because$	\because	$\therefore$	\therefore
$\nless$	\nless	$\ngtr$	\ngtr	$\lessdot$	\lessdot	$\gtrdot$	\gtrdot
$\lessgtr$	\lessgtr	$\gtrless$	\gtrless	$\lesseqgtr$	\lesseqgtr	$\gtreqless$	\gtreqless
$\subseteqq$	\subseteqq	$\supseteqq$	\supseteqq	$\subsetneqq$	\subsetneqq	$\supsetneqq$	\supsetneqq

数学符号与字体

- 箭头与长等号

箭头

$\leftarrow$	\leftarrow	$\longleftarrow$	\longleftarrow
$\rightarrow$	\rightarrow	$\longrightarrow$	\longrightarrow
$\leftrightarrow$	\leftrightarrow	$\longleftrightarrow$	\longleftrightarrow
$\Leftarrow$	\Leftarrow	$\Longleftarrow$	\Longleftarrow
$\Rightarrow$	\Rightarrow	$\Longrightarrow$	\Longrightarrow
$\Leftrightarrow$	\Leftrightarrow	$\Longleftrightarrow$	\Longleftrightarrow
$\mapsto$	\mapsto	$\longmapsto$	\longmapsto
$\nearrow$	\nearrow	$\searrow$	\searrow
$\swarrow$	\swarrow	$\nwarrow$	\nwarrow
$\leftharpoonup$	\leftharpoonup	$\rightharpoonup$	\rightharpoonup
$\leftharpoondown$	\leftharpoondown	$\rightharpoondown$	\rightharpoondown
$\rightleftharpoons$	\rightleftharpoons	$\iff$	\iff (bigger space)

数学符号与字体

- 箭头与长等号

amssymb 箭头

⇠	\dashleftarrow	⇢	\dashrightarrow
↺	\circlearrowleft	↻	\circlearrowright
⇆	\leftrightarrows	⇄	\leftrightarrows
↚	\nleftarrow	⇍	\nLeftarrow
↛	\nrightarrow	⇏	\nRightarrow
↮	\nleftrightarrow	⇎	\nLeftrightarrow

数学符号与字体

- 其他符号

其他符号

…	\dots	⋯	\cdots	⋮	\vdots	⋱	\ddots
∀	\forall	∃	\exists	ℜ	\Re	ℵ	\aleph
∠	\angle	∞	\infty	△	\triangle	∇	\nabla
ℏ	\hbar	ı	\imath	ȷ	\jmath	ℓ	\ell
♠	\spadesuit	♡	\heartsuit	♣	\clubsuit	♢	\diamondsuit
♭	\flat	♮	\natural	♯	\sharp		

非数学符号:

£	\pounds	§	\S	©	\copyright	¶	\P
†	\dag	‡	\ddag	®	\textregistered		

amssymb 其他符号

□	\square	■	\blacksquare	ℏ	\hbar
★	\bigstar	▲	\blacktriangle	▼	\blacktriangledown
◊	\lozenge	⧫	\blacklozenge	∡	\measuredangle
℧	\mho	∅	\varnothing	ð	\eth

公式排版练习

$$\mathbf{H}_{ij} \succ \left(\underbrace{\begin{bmatrix} \alpha_{ij} & -\alpha_{ij} \\ -\alpha_{ij} & \alpha_{ij} \end{bmatrix}}_{\text{PSD Laplacian term}} - \underbrace{\frac{p}{2}\theta_{ij}^{p-1} \begin{bmatrix} \mathbf{I}_3 & \mathbf{0} \\ \mathbf{0} & \mathbf{I}_3 \end{bmatrix}}_{\text{non-PSD curvature term}} \right) \otimes \mathbf{I}_3$$

$$\begin{aligned}
&\min_{\theta_i} \mathcal{L}(\theta_i - \alpha \nabla_{\theta_i} \mathcal{L}(\theta_i, \mathcal{D}_i), \mathcal{D}_{i+1}) \\
&\approx \min_{\theta_i} \mathcal{L}(\theta_i, \mathcal{D}_{i+1}) - \alpha \nabla_{\theta_i} \mathcal{L}(\theta_i, \mathcal{D}_i) \cdot \nabla_{\theta_i} \mathcal{L}(\theta_i, \mathcal{D}_{i+1}) \\
&\quad + H_{\theta_i} \cdot [\alpha \nabla_{\theta_i} \mathcal{L}(\theta_i, \mathcal{D}_i)]^2 + \dots \\
&\approx \min_{\theta_i} \mathcal{L}(\theta_i, \mathcal{D}_{i+1}) - \alpha \left\langle \nabla_{\theta_i} \mathcal{L}(\theta_i, \mathcal{D}_i), \nabla_{\theta_i} \mathcal{L}(\theta_i, \mathcal{D}_{i+1}) \right\rangle
\end{aligned}$$

$$\begin{aligned}
&\max_{\phi_S, \phi_I} \min_{\theta_S, \theta_I} \mathcal{L}_r(G_{\theta_S}^{S \to I}, \mathcal{S}_p, \mathcal{I}_p) + \lambda_1 \mathcal{L}_r(G_{\theta_I}^{I \to S}, \mathcal{I}_p, \mathcal{S}_p) \\
&+ \lambda_2 \mathcal{L}_a(G_{\theta_S}^{S \to I}, D_{\phi_I}^I, \mathcal{S}_{p,u}) + \lambda_3 \mathcal{L}_a(G_{\theta_I}^{I \to S}, D_{\phi_S}^S, \mathcal{I}_{p,u}) \\
&+ \lambda_4 \mathcal{L}_c(G_{\theta_S}^{S \to I}, G_{\theta_I}^{I \to S}, \mathcal{S}_{p,u}) + \lambda_5 \mathcal{L}_c(G_{\theta_I}^{I \to S}, G_{\theta_S}^{S \to I}, \mathcal{I}_{p,u})
\end{aligned}$$

公式排版练习

$$
\begin{aligned}
e^2 &= e^2(R, \mathbf{t}; \mathbf{w}, X, Y) \\
&= \sum_{(i,j)\in\mathcal{M}} \tilde{w}_{(i,j)} (\mathbf{y}_j - (R\mathbf{x}_i + \mathbf{t}))^2 \\
&= \mathrm{Tr}\left((Y - RX - \mathbf{t}\mathbf{1}^T) W (Y - RX - \mathbf{t}\mathbf{1}^T)^T \right)
\end{aligned}
$$

$$
S^+(\mathbf{x}) = \left[\sum_j W_j \left[1 - C_j^+(\mathbf{x}) \right]_{[0,1]} \right]_{[0,1]} \begin{cases} = 1 & \approx \text{in} \\ [0,1) & \approx \text{out} \end{cases}
$$

$$
f(\boldsymbol{p}_i) = \begin{cases} \text{False} & \|\boldsymbol{p}_i - \boldsymbol{q}_i\|_2 > D(\boldsymbol{q}_i) \\ \text{True} & \text{otherwise} \end{cases}
$$

$$
D(\boldsymbol{q}_i) = \max_{\boldsymbol{q}_m, \boldsymbol{q}_n \in N(\boldsymbol{q}_i)} \min \|\boldsymbol{q}_m - \boldsymbol{q}_n\|_2, m \neq n
$$

An Invitation to LaTeX

Xiang Gao, Lecturer

E-mail: xgao@ouc.edu.cn | Web: https://ouc-xgao.github.io/

College of Engineering, Ocean University of China

课程回顾

- LaTeX公式
  - 行内与行间公式
    - 行内公式，行间公式
  - 基本命令
    - 上下标与虚位
    - 分式、根式与堆叠
    - 累加与累积
    - 矩阵与省略号
    - **分段函数与联立方程**
    - **多行公式及其编号**

课程回顾

- LaTeX公式
  - 数学符号与字体
    - 字体
    - 字号
    - 定界符
    - 希腊字母
    - 二元运算符
    - 二元关系符
    - 箭头与长等号
    - 其他符号

公式截图识别

- Snip

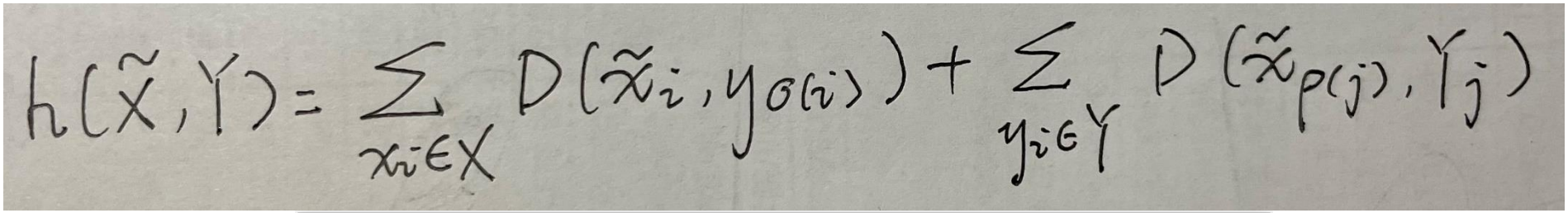
$h(\tilde{x}, Y) = \sum_{x_i \in X} D(\tilde{x}_i, y_{G(i)}) + \sum_{y_i \in Y} D(\tilde{x}_{p(j)}, Y_j)$

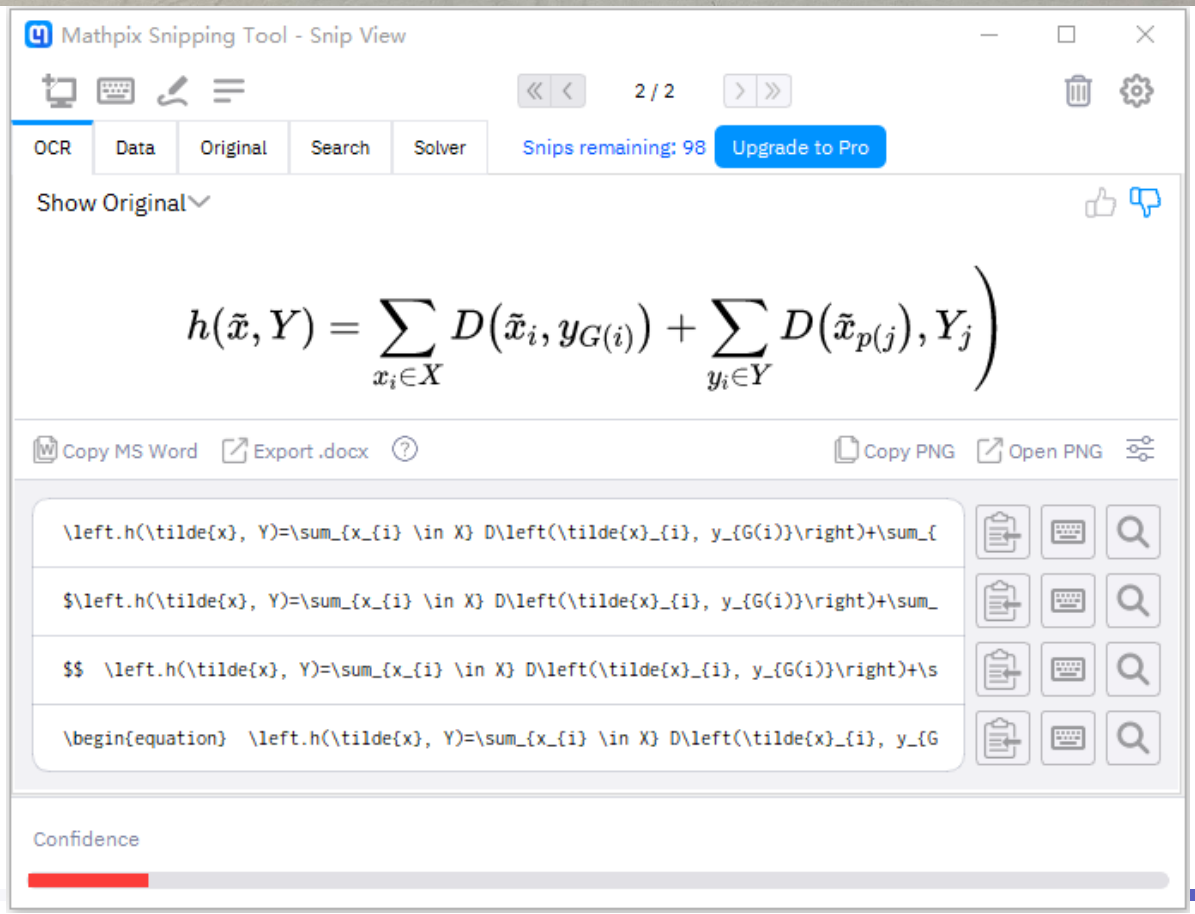
Mathpix Snipping Tool - Snip View
2 / 2
OCR
Data
Original
Search
Solver
Snips remaining: 98
Upgrade to Pro
Show Original
$$h(\tilde{x}, Y) = \sum_{x_i \in X} D(\tilde{x}_i, y_{G(i)}) + \sum_{y_i \in Y} D(\tilde{x}_{p(j)}, Y_j)$$
Copy MS Word
Export .docx
Copy PNG
Open PNG
\left.h(\tilde{x}, Y)=\sum_{x_{i} \in X} D\left(\tilde{x}_{i}, y_{G(i)}\right)+\sum_{
$\left.h(\tilde{x}, Y)=\sum_{x_{i} \in X} D\left(\tilde{x}_{i}, y_{G(i)}\right)+\sum_
$$ \left.h(\tilde{x}, Y)=\sum_{x_{i} \in X} D\left(\tilde{x}_{i}, y_{G(i)}\right)+\s
\begin{equation} \left.h(\tilde{x}, Y)=\sum_{x_{i} \in X} D\left(\tilde{x}_{i}, y_{G
Confidence

课程大纲

- LaTeX一览
- LaTeX基础
- LaTeX公式
- LaTeX进阶
  - 自定义命令
  - 自定义图表
  - BibTeX参考文献
  - 算法排版

自定义命令

- 自定义命令
  - \newcommand{命令名称}[参数个数][首参数默认值]{具体定义}
  - \newcommand{\loves}[3][loves]{#2#1#3}
  - \loves{Jack}{Rose}　　Jack loves Rose
  - \loves[hates]{Jack}{Rose}　Jack hates Rose

自定义图表

- 三线表
  - booktabs宏包提供\toprule, \midrule与\bottomrule命令来绘制三线表
  - 需要更多横线可以通过\midrule添加
  - 从i到j列的横线通过\cmidrule{i-j}添加

```
\begin{tabular}{cccc}
\toprule
& \multicolumn{3}{c}{Numbers} \\
\cmidrule{2-4}
& 1 & 2 & 3 \\
\midrule
Alphabet & A & B & C \\
Roman & I & II& III \\
\bottomrule
\end{tabular}
```

	Numbers		
	1	2	3
Alphabet	A	B	C
Roman	I	II	III

自定义图表

- 彩色表
  - 彩色表格依靠colortbl宏包，它会调用array和color宏包（嵌套包含）
  - 其命令\columncolor{color}，\rowcolor{color}，以及\cellcolor{color}分别表示给表格**某**列，**当前**行，以及**当前**单元格加背景色color

```
1  \begin{table}[htbp]
2  \centering
3  \begin{tabular}{l>{\columncolor{yellow}}ll}
4  \hline
5  \rowcolor{magenta}OS & Release & Editor \\
6  Windows & MikTeX & TexMakerX \\
7  \rowcolor{red}Unix/Linux & \cellcolor{cyan}teTeX & Kile \\
8  Mac OS & MacTeX & TeXShop \\
9  \rowcolor{orange}General & TeX Live & TeXworks \\
10 \hline
11 \end{tabular}
12 \end{table}
```

OS	Release	Editor
Windows	MikTeX	TexMakerX
Unix/Linux	teTeX	Kile
Mac OS	MacTeX	TeXShop
General	TeX Live	TeXworks

自定义图表

- 彩色表
  - 另外，可以通过加载xcolor宏包时添加table选项来调用colortbl宏包：
  - \usepackage[table]{xcolor}
  - xcolor宏包支持\rowcolors{}命令，需将该命令置于表格开始之前

```
% 表线为单横，从第2行开始，奇数行绿，偶数行青
\rowcolors[\hline]{2}{green}{cyan}
\begin{tabular}...
```

OS	Release	Editor
Windows	MikTeX	TexMakerX
Unix/Linux	teTeX	Kile
Mac OS	MacTeX	TeXShop
General	TeX Live	TeXworks

```
\begin{table}[htbp]
\centering
\rowcolors{2}{blue!20}{blue!10}
\begin{tabular}{lll} \hline
OS & Release & Editor \\
Windows & MikTeX & TexMakerX \\
Unix/Linux & teTeX & Kile \\
Mac OS & MacTeX & TeXShop \\
General & TeX Live & TeXworks \\ \hline
\end{tabular}
\end{table}
```

自定义图表

- 排版练习

	Algorithm	higher is better $= 0$	≤ 1	≤ 2	≤ 4	lower is better MAE	RMSE
I*	Mean Local Ratio ($\sigma = 2$)	0.222	0.578	0.776	0.932	2.181	5.184
I*	Mean Local Log-Ratio ($\sigma = 2$)	0.222	0.579	0.776	0.932	2.176	5.178
I*	Mean Local Norm-Dist-Sq ($\sigma = 2$)	0.221	0.576	0.773	0.928	2.202	5.097
I*	Mean Local Ratio ($\sigma = 4$)	0.212	0.565	0.773	0.940	1.923	3.920
I*	Mean Local Log-Ratio ($\sigma = 4$)	0.213	0.566	0.774	0.941	1.916	3.917
I*	Wavelet Sum ($\ell = 3$)	0.194	0.520	0.731	0.922	2.019	3.558
I*	Mean Wavelet Log-Ratio ($\ell = 3$)	0.185	0.504	0.718	0.922	2.003	3.239
I*	**Our Model**	**0.251**	**0.610**	**0.809**	**0.957**	**1.570**	**2.529**

BibTeX参考文献

- BibTeX使用
  - BibTeX通过单独的.bib拓展名文件管理文献，使多文档方便地共享一份文献列表成为可能。使用BibTeX时需要确保如下几点：
    - 文档定义了\bibliographystyle{}类型。LaTeX预定义地类型包括下面几种：
      - plain：按照作者字母顺序排序
      - unsrt：按照引用顺序排序
      - alpha：按照作者名称和出版年份排序
    - 在文档中插入了\cite{}命令
    - 在参考文献列表位置插入了**\bibliography{bib}**命令

BibTeX参考文献

- BibTeX使用
  - 简单例子

```
\bibliographystyle{plain}
\begin{document}
    ...
    ... and published here\cite{Smith93TRB}.
    ...
    \bibliography{myBib}
\end{document}
```

  - 在对应的myBib.bib文件中，需要有类似如下条目

```
% 如果引用期刊
@article{Smith1993TRB,
    author = {作者，多个作者用and 连接},
    title = {标题},
    journal = {期刊名},
    volume = {卷20},
    number = {页码},
    year = {年份},
    abstract = {摘要，引用的时候自己参考，非必须}}
% 如果引用书籍
@book{Smith1993TRB,
    author ="作者",
    year="年份2008",
    title="书名",
    publisher ="出版社名称"}
```

BibTeX参考文献

- bib文件查找方式
  - 搜索引擎
    - Google Scholar
    - Microsoft Academic
    - 百度学术
    - ~~中国知网~~
  - 学术网站
    - CVF
    - ResearchGate
    - dblp

BibTeX参考文献

- bib文件查找方式
  - 搜索引擎
    - **Google Scholar**
    - Microsoft Academic
    - 百度学术
    - ~~中国知网~~
  - 学术网站
    - CVF
    - ResearchGate
    - dblp

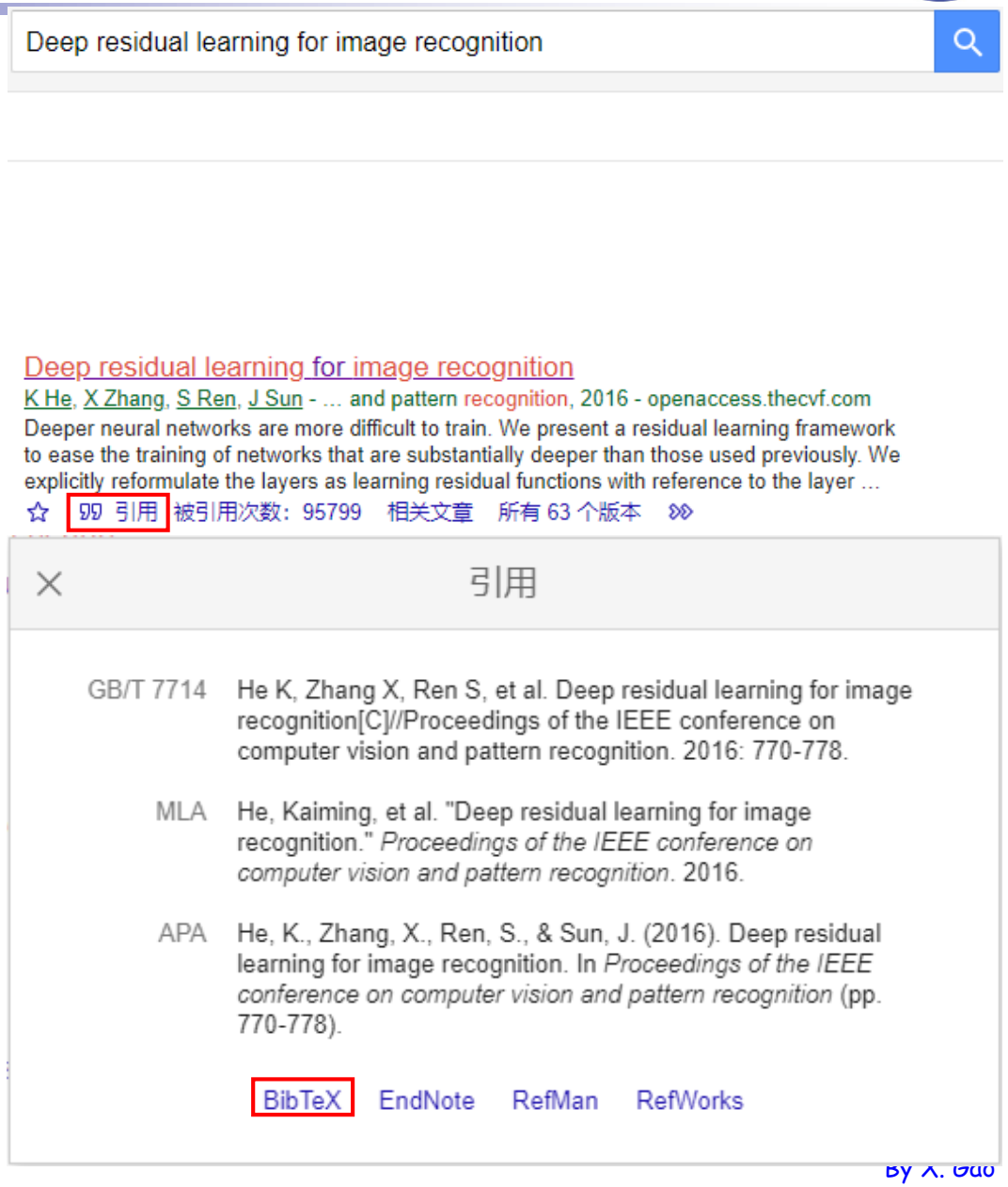

BibTeX参考文献

- bib文件查找方式
  - 搜索引擎
    - Google Scholar
    - **Microsoft Academic**
    - 百度学术
    - ~~中国知网~~
  - 学术网站
    - CVF
    - ResearchGate
    - dblp

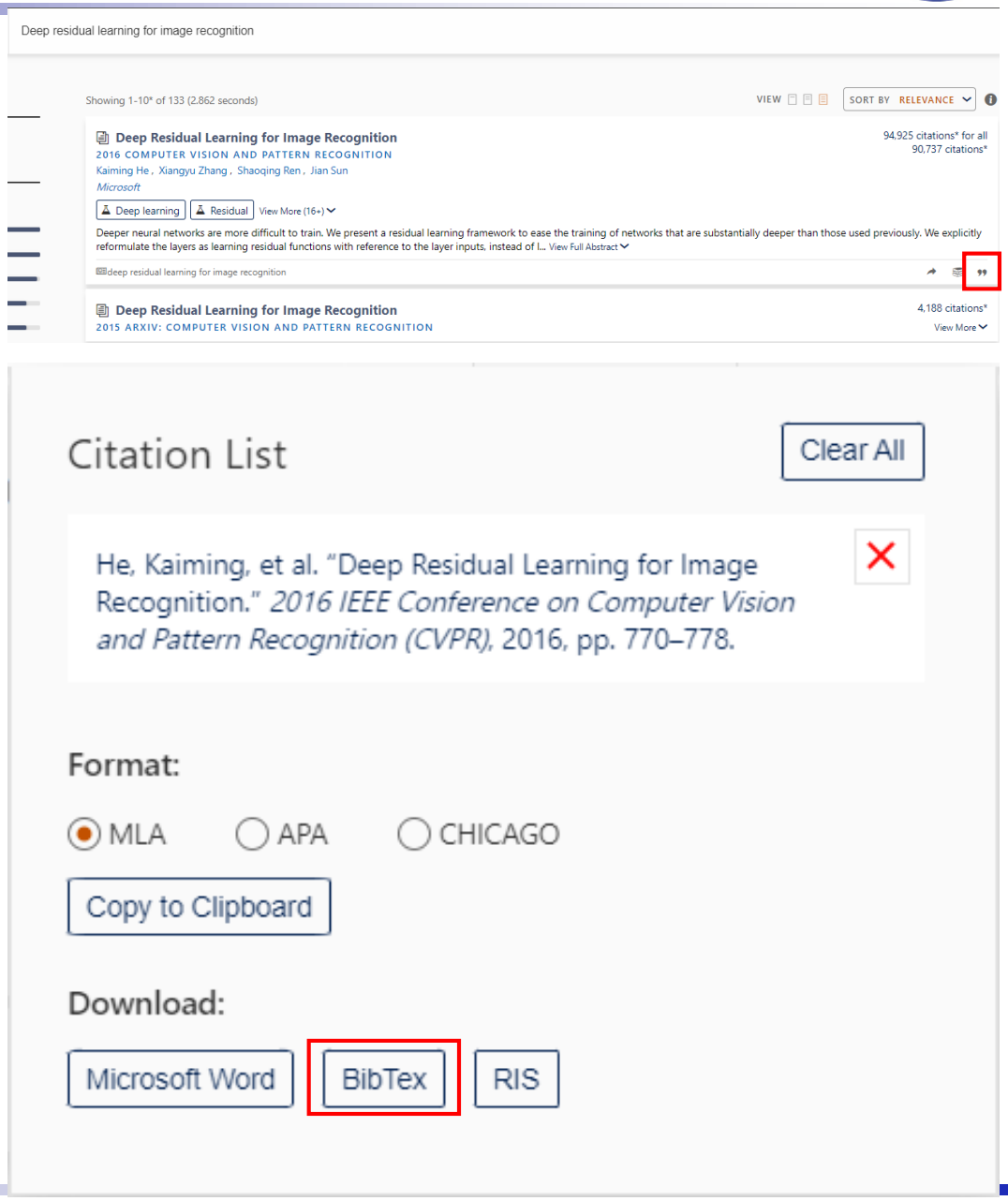

BibTeX参考文献

- bib文件查找方式
  - 搜索引擎
    - Google Scholar
    - Microsoft Academic
    - **百度学术**
    - ~~中国知网~~
  - 学术网站
    - CVF
    - ResearchGate
    - dblp

BibTeX参考文献

- bib文件查找方式
  - 搜索引擎
    - Google Scholar
    - Microsoft Academic
    - 百度学术
    - ~~中国知网~~
  - 学术网站
    - **CVF**
    - ResearchGate
    - dblp

Deep Residual Learning for Image Recognition

Kaiming He, Xiangyu Zhang, Shaoqing Ren, Jian Sun; Proceedings of the IEEE Conference on Computer Vision and Pattern Recognition (CVPR), 2016, pp. 770-778

Abstract

Deeper neural networks are more difficult to train. We present a residual learning framework to ease the training of networks that are substantially deeper than those used previously. We explicitly reformulate the layers as learning residual functions with reference to the layer inputs, instead of learning unreferenced functions. We provide comprehensive empirical evidence showing that these residual networks are easier to optimize, and can gain accuracy from considerably increased depth. On the ImageNet dataset we evaluate residual nets with a depth of up to 152 layers---8x deeper than VGG nets but still having lower complexity. An ensemble of these residual nets achieves 3.57% error on the ImageNet test set. This result won the 1st place on the ILSVRC 2015 classification task. We also present analysis on CIFAR-10 with 100 and 1000 layers. The depth of representations is of central importance for many visual recognition tasks. Solely due to our extremely deep representations, we obtain a 28% relative improvement on the COCO object detection dataset. Deep residual nets are foundations of our submissions to ILSVRC & COCO 2015 competitions, where we also won the 1st places on the tasks of ImageNet detection, ImageNet localization, COCO detection, and COCO segmentation.

Related Material

[pdf] [supp] [video] [bibtex]

BibTeX参考文献

- bib文件查找方式
  - 搜索引擎
    - Google Scholar
    - Microsoft Academic
    - 百度学术
    - ~~中国知网~~
  - 学术网站
    - CVF
    - **ResearchGate**
    - dblp

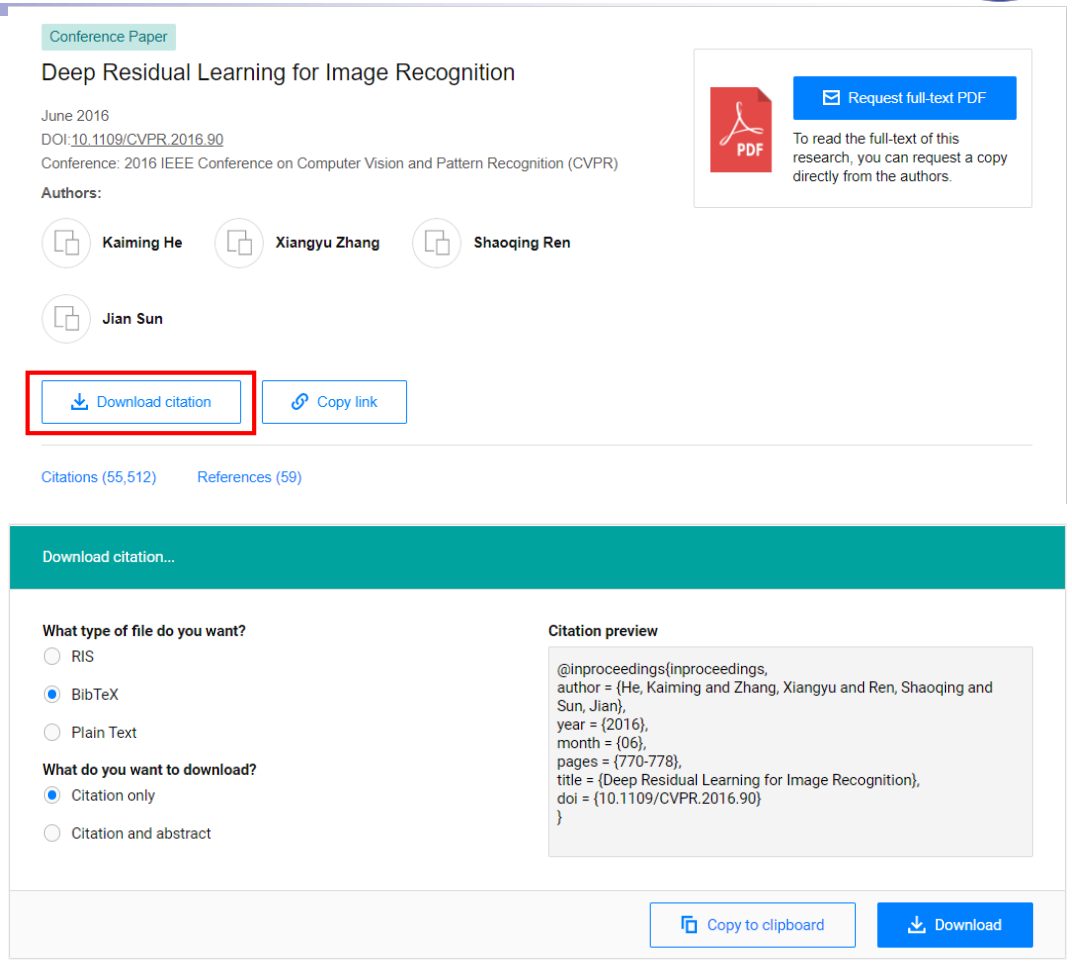

BibTeX参考文献

- bib文件查找方式
  - 搜索引擎
    - Google Scholar
    - Microsoft Academic
    - 百度学术
    - ~~中国知网~~
  - 学术网站
    - CVF
    - ResearchGate
    - **dblp**

BibTeX参考文献

- bib文件查找方式
  - **出版社官网**
    - **IEEE**
    - **Elsevier**
    - **Springer**
    - **ACM**
    - **Wiley**
  - 个人主页
    - Shaoqing Ren
    - Georgia Gkioxari
    - Shanzhe Wu

BibTeX参考文献

- bib文件查找方式
  - **出版社官网**
    - **IEEE**
    - Elsevier
    - Springer
    - ACM
    - Wiley
  - 个人主页
    - Shaoqing Ren
    - Georgia Gkioxari
    - Shanzhe Wu

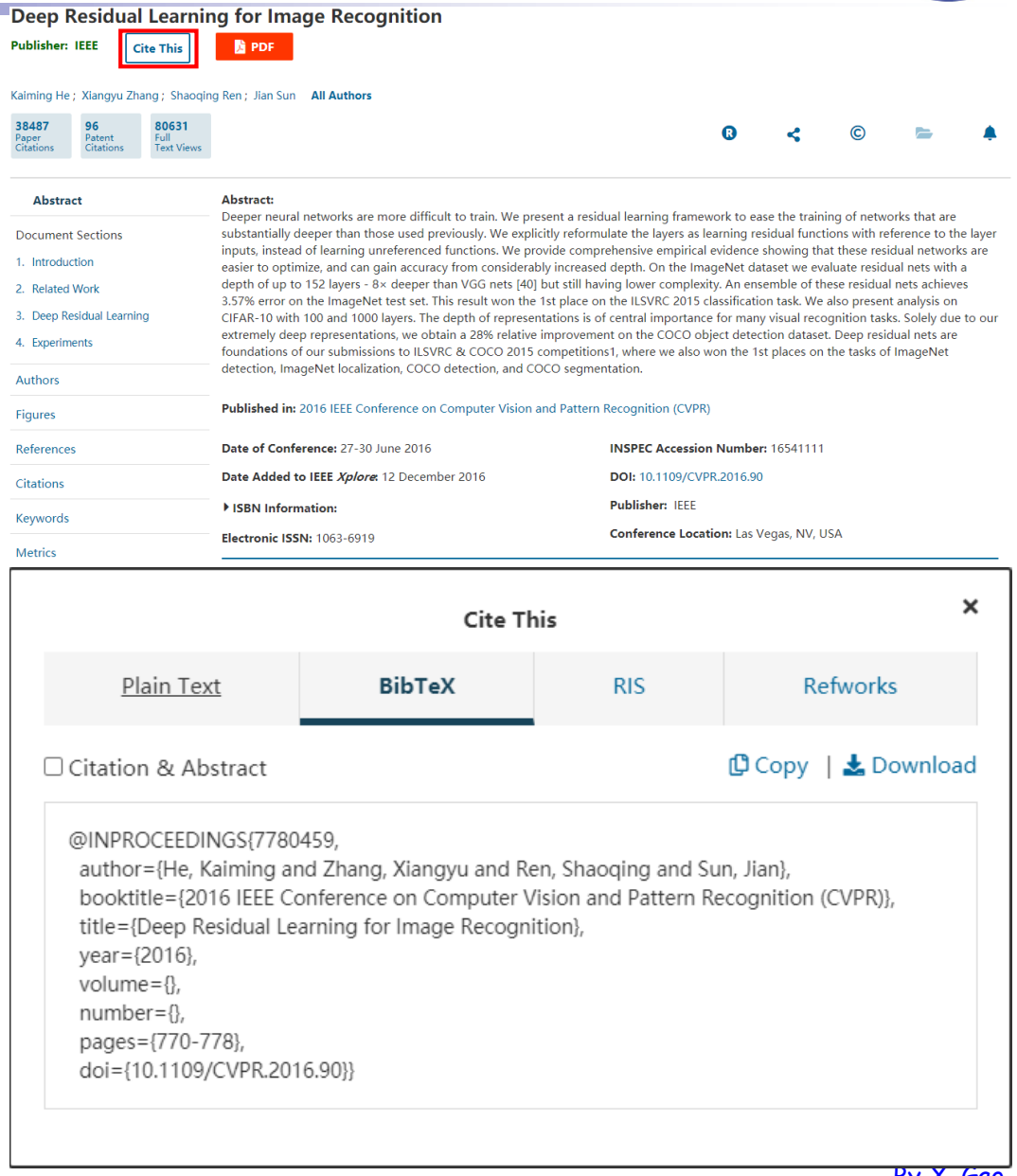

BibTeX参考文献

- bib文件查找方式
  - **出版社官网**
    - **IEEE**
    - Elsevier
    - Springer
    - ACM
    - Wiley
  - 个人主页
    - **Shaoqing Ren**
    - Georgia Gkioxari
    - Shanzhe Wu

Deep Residual Learning for Image Recognition,
Kaiming He, Xiangyu Zhang, **Shaoqing Ren**, Jian Sun .
IEEE Conference on Computer Vision and Pattern Recognition (**CVPR**), 2016 *(Oral)*, *CVPR Best Paper*
Paper / Bibtex

```
@inproceedings{he15deepresidual,
  Author    = {Kaiming He and
               Xiangyu Zhang and
               Shaoqing Ren and
               Jian Sun},
  Title     = {Deep Residual Learning for Image Recognition},
  Booktitle = {arXiv prepring arXiv:1506.01497},
  Year      = {2015}}
```

ILSVRC 2015 & COCO 2015 - we won the 1st places in ImageNet classification, ImageNet detection, ImageNet localization, COCO detection, and COCO segmentation with ResNet and Faster R-CNN!

Shaoqing Ren

FOLLOW

NIO
Verified email at nio.com - Homepage

Computer Vision Deep Learning Autonomous Driving

TITLE	CITED BY	YEAR
Deep residual learning for image recognition K He, X Zhang, S Ren, J Sun Proceedings of the IEEE conference on computer vision and pattern ...	58520	2016
Faster r-cnn: Towards real-time object detection with region proposal networks S Ren, K He, R Girshick, J Sun Conference on Neural Information Processing Systems (NIPS 2015)	22601	2015
Delving deep into rectifiers: Surpassing human-level performance on imagenet classification K He, X Zhang, S Ren, J Sun IEEE International Conference on Computer Vision (ICCV 2015)	9498	2015
Spatial pyramid pooling in deep convolutional networks for visual recognition K He, X Zhang, S Ren, J Sun IEEE transactions on pattern analysis and machine intelligence 37 (9), 1904-1916	4950	2015
Identity mappings in deep residual networks K He, X Zhang, S Ren, J Sun European conference on computer vision, 630-645	4355	2016
Face Alignment at 3000 FPS via Regressing Local Binary Features S Ren, X Cao, Y Wei, J Sun IEEE Conference on Computer Vision and Pattern Recognition (CVPR 2014)	877	2014
Joint cascade face detection and alignment D Chen, S Ren, Y Wei, X Cao, J Sun European conference on computer vision, 109-122	358	2014
Instance-sensitive fully convolutional networks J Dai, K He, Y Li, S Ren, J Sun European Conference on Computer Vision, 534-549	289	2016
Object detection networks on convolutional feature maps S Ren, K He, R Girshick, X Zhang, J Sun IEEE transactions on pattern analysis and machine intelligence 39 (7), 1476-1481	278	2016
Global refinement of random forest S Ren, X Cao, Y Wei, J Sun IEEE Conference on Computer Vision and Pattern Recognition (CVPR 2015), 723-730	87	2015

Cited by

	All	Since 2015
Citations	101893	101634
h-index	12	12
i10-index	12	12

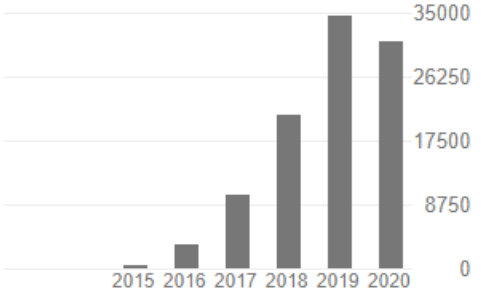

Co-authors

Kaiming He
Research Scientist, Facebook AI...

Jian Sun
Chief Scientist/Managing Directo...

Xiangyu Zhang
Research Leader, MEGVII Techn...

Ross Girshick
Research Scientist, Facebook AI...

Xudong Cao
CEO at Momenta.ai

Yichen Wei
Megvii Research Shanghai

Dong Chen
Principal Research Manager, Mic...

Jifeng Dai
Executive Research Director, Se...

Shaoqing Ren

关注

NIO
在 nio.com 的电子邮件经过验证 - 首页
Computer Vision Deep Learning Autonomous Driving

创建我的个人资料

标题	引用次数	年份
Deep residual learning for image recognition K He, X Zhang, S Ren, J Sun Proceedings of the IEEE conference on computer vision and pattern ...	96639	2016
Faster r-cnn: Towards real-time object detection with region proposal networks S Ren, K He, R Girshick, J Sun Conference on Neural Information Processing Systems (NIPS 2015)	36070	2015
Delving deep into rectifiers: Surpassing human-level performance on imagenet classification K He, X Zhang, S Ren, J Sun IEEE International Conference on Computer Vision (ICCV 2015)	13666	2015
Spatial pyramid pooling in deep convolutional networks for visual recognition K He, X Zhang, S Ren, J Sun IEEE transactions on pattern analysis and machine intelligence 37 (9), 1904-1916	7167	2015
Identity mappings in deep residual networks K He, X Zhang, S Ren, J Sun European conference on computer vision, 630-645	6575	2016
Face Alignment at 3000 FPS via Regressing Local Binary Features S Ren, X Cao, Y Wei, J Sun IEEE Conference on Computer Vision and Pattern Recognition (CVPR 2014)	1041	2014
Joint cascade face detection and alignment D Chen, S Ren, Y Wei, X Cao, J Sun European conference on computer vision, 109-122	455	2014
Object detection networks on convolutional feature maps S Ren, K He, R Girshick, X Zhang, J Sun IEEE transactions on pattern analysis and machine intelligence 39 (7), 1476-1481	375	2016
Instance-sensitive fully convolutional networks J Dai, K He, Y Li, S Ren, J Sun European Conference on Computer Vision, 534-549	369	2016
Global refinement of random forest S Ren, X Cao, Y Wei, J Sun IEEE Conference on Computer Vision and Pattern Recognition (CVPR 2015), 723-730	103	2015
D eep re sidu al le arning for i ma ge recognition ZXY HE KM, SQ REN T he 2 (016), 770-77	52	

引用次数

	总计	2016 年至今
引用	162512	159530
h 指数	11	11
i10 指数	11	11

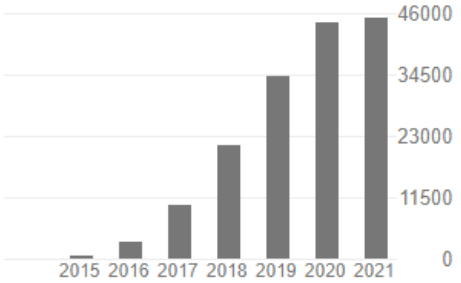

合著作者

Jian Sun
Chief Scientist/Managing Directo...

Kaiming He
Research Scientist, Facebook AI...

Xiangyu Zhang
Principal Researcher, MEGVII Te...

Ross Girshick
Research Scientist, Facebook AI...

Xudong Cao
CEO at Momenta.ai

Yichen Wei
Megvii Research Shanghai

Dong Chen
Principal Research Manager, Mic...

Jifeng Dai
Executive Research Director, Se...

算法排版

- algorithm2e宏包备选项
  - ruled
    - 标题显示在算法表上面
  - linesnumbered
    - 算法显示行号
  - vlined
    - 去掉end，作用域线内折
- algorithm2e宏包常用命令
  - 右图

代码	含义
\;	在行末添加分号，并自动换行
\caption{}	插入标题
\KwData {输入信息}	效果为：“Data:输入信息”
\KwIn {输入信息}	效果为：“In: 输入信息”
\KwOut {输出信息}	效果为：“Out: 输出信息”
\KwResult {输出信息}	效果为：“Result: 输出信息”
\For {条件}{循环语句}	for 条件 do 循环语句 end
\If {条件}{肯定语句}	if 条件 then 肯定语句 end
\While {条件}{循环语句}	while 条件 do 循环语句 end
\tcc{注释}	/* 注释 */
\tcp{注释}	//注释

\eIf {条件}{肯定语句}{否定语句}	if 条件 then
	肯定语句
	else
	否定语句
	end

算法排版

- 算法排版示例

```
\documentclass{article}
\usepackage[ruled,linesnumbered]{algorithm2e}
\begin{document}
\begin{algorithm}
\caption{Simulation-optimization heuristic}
\KwData{current period $t$, initial inventory $I_{t-1}$, initial capital $B_{t-1}$, demand samples}
\KwResult{Optimal order quantity $Q^{\ast}_{t}$}
$r\leftarrow t$\;
$\Delta B^{\ast}\leftarrow -\infty$\;
\While{$\Delta B\leq \Delta B^{\ast}$ and $r\leq T$}
{
        $Q\leftarrow\arg\max_{Q\geq 0}\Delta B^{Q}_{t,r}(I_{t-1},B_{t-1})$\;
        $\Delta B\leftarrow \Delta B^{Q}_{t,r}(I_{t-1},B_{t-1})/(r-t+1)$\;
        \If{$\Delta B\geq \Delta B^{\ast}$}
        {
                $Q^{\ast}\leftarrow Q$\;
                $\Delta B^{\ast}\leftarrow \Delta B$\;
        }
        $r\leftarrow r+1$\;
}
\end{algorithm}
\end{document}
```

Algorithm 1: Simulation-optimization heuristic

Data: current period t, initial inventory I_{t-1}, initial capital B_{t-1}, demand samples

Result: Optimal order quantity Q_t^*

$r \leftarrow t$;
$\Delta B^* \leftarrow -\infty$;
while $\Delta B \leq \Delta B^*$ *and* $r \leq T$ **do**
  $Q \leftarrow \arg\max_{Q\geq 0} \Delta B^{Q}_{t,r}(I_{t-1}, B_{t-1})$;
  $\Delta B \leftarrow \Delta B^{Q}_{t,r}(I_{t-1}, B_{t-1})/(r-t+1)$;
  if $\Delta B \geq \Delta B^*$ **then**
    $Q^* \leftarrow Q$;
    $\Delta B^* \leftarrow \Delta B$;
  end
  $r \leftarrow r+1$;
end

算法排版

- 算法排版示例

```
\documentclass{article}
\usepackage[ruled,linesnumbered,vlined]{algorithm2e}
\begin{document}
\begin{algorithm}
\caption{Simulation-optimization heuristic}
\KwIn{current period $t$, initial inventory $I_{t-1}$, initial capital $B_{t-1}$, demand samples}
\KwOut{Optimal order quantity $Q^{\ast}_{t}$}
$r\leftarrow t$\;
$\Delta B^{\ast}\leftarrow -\infty$\;
\For{$\Delta B\leq \Delta B^{\ast}$ and $r\leq T$}
{
    $Q\leftarrow\arg\max_{Q\geq 0}\Delta B^{Q}_{t,r}(I_{t-1},B_{t-1})$\;
    $\Delta B\leftarrow \Delta B^{Q}_{t,r}(I_{t-1},B_{t-1})/(r-t+1)$\;
    \If{$\Delta B\geq \Delta B^{\ast}$}
    {
        $Q^{\ast}\leftarrow Q$\;
        $\Delta B^{\ast}\leftarrow \Delta B$\;
    }
    $r\leftarrow r+1$\;
}
\end{algorithm}
\end{document}
```

Algorithm 1: Simulation-optimization heuristic

Input: current period t, initial inventory I_{t-1}, initial capital B_{t-1}, demand samples

Output: Optimal order quantity Q_t^*

$r \leftarrow t$;
$\Delta B^* \leftarrow -\infty$;
for $\Delta B \leq \Delta B^*$ *and* $r \leq T$ **do**
    $Q \leftarrow \arg\max_{Q\geq 0} \Delta B^Q_{t,r}(I_{t-1}, B_{t-1})$;
    $\Delta B \leftarrow \Delta B^Q_{t,r}(I_{t-1}, B_{t-1})/(r-t+1)$;
    if $\Delta B \geq \Delta B^*$ **then**
        $Q^* \leftarrow Q$;
        $\Delta B^* \leftarrow \Delta B$;
    $r \leftarrow r+1$;

算法排版

- 算法排版练习

Algorithm 1 Optimization with Filter Method

Require: Initial solution $\mathbf{x}^0$, filter margin α, `max_iter`

Initialization: $t \leftarrow 0, \mathcal{F} \leftarrow \emptyset, \mathbb{F} \leftarrow \emptyset$
while `true` and $t <$ `max_iter` **do**
  if $\mathbf{x}^t$ is stationary **then**
    break;
  end if
  $\tilde{f} \leftarrow f_t - \alpha h_t; \tilde{h} \leftarrow h_t - \alpha h_t$
  $\mathcal{F} \leftarrow \mathcal{F} \cup \{(\tilde{f}, \tilde{h})\}$
  $\mathbf{F}_{t+1} \leftarrow \{\mathbf{x} | f(\mathbf{x}) \geq \tilde{f}, h(\mathbf{x}) \geq \tilde{h}\}$
  $\mathbb{F} \leftarrow \mathbb{F} \cup \mathbf{F}_{t+1}$
  Compute $\mathbf{x}^{t+1} \notin \mathbb{F}$ (Sec. 5.2.1 and 5.2.2)
  if $f(\mathbf{x}^{t+1}) < f(\mathbf{x}^t)$ **then**
    $\mathcal{F} \leftarrow \mathcal{F} \setminus \{(\tilde{f}, \tilde{h})\}; \mathbb{F} \leftarrow \mathbb{F} \setminus \mathbf{F}_{t+1}$
  end if
  $t \leftarrow t + 1$
end while
return $\mathbf{x}^t$

Notes on Thesis Writing

Xiang Gao, Lecturer

E-mail: xgao@ouc.edu.cn | Web: https://ouc-xgao.github.io/

College of Engineering, Ocean University of China

提纲

- 论文题目
- 整体布局
- 常见问题
- 注重细节
- 结束语
- 参考资料

论文题目

- 基本要领
  - 措辞简单明了，通俗易懂
  - 含义明确，不宜太大，但能概括全文
  - 尽量有特色，不宜太长
- 举例
  - 统计机器翻译新方法研究 😔太大了
  - 面向×××的若干问题研究 😔太泛了
  - 融合源语言句法知识的统计翻译模型研究 😊

整体布局

- 基本要领
  - 开门见山，尽早破题
  - 全文各部分是有机联系的整体，构成一个完整的“故事 (Story)”
  - 切忌将已发表的几篇论文简单地拼凑、堆叠在一起，各章内容互不相干
  - 主题鲜明，重点突出，所有章节的内容均围绕主题展开

整体布局

- 阐述方式

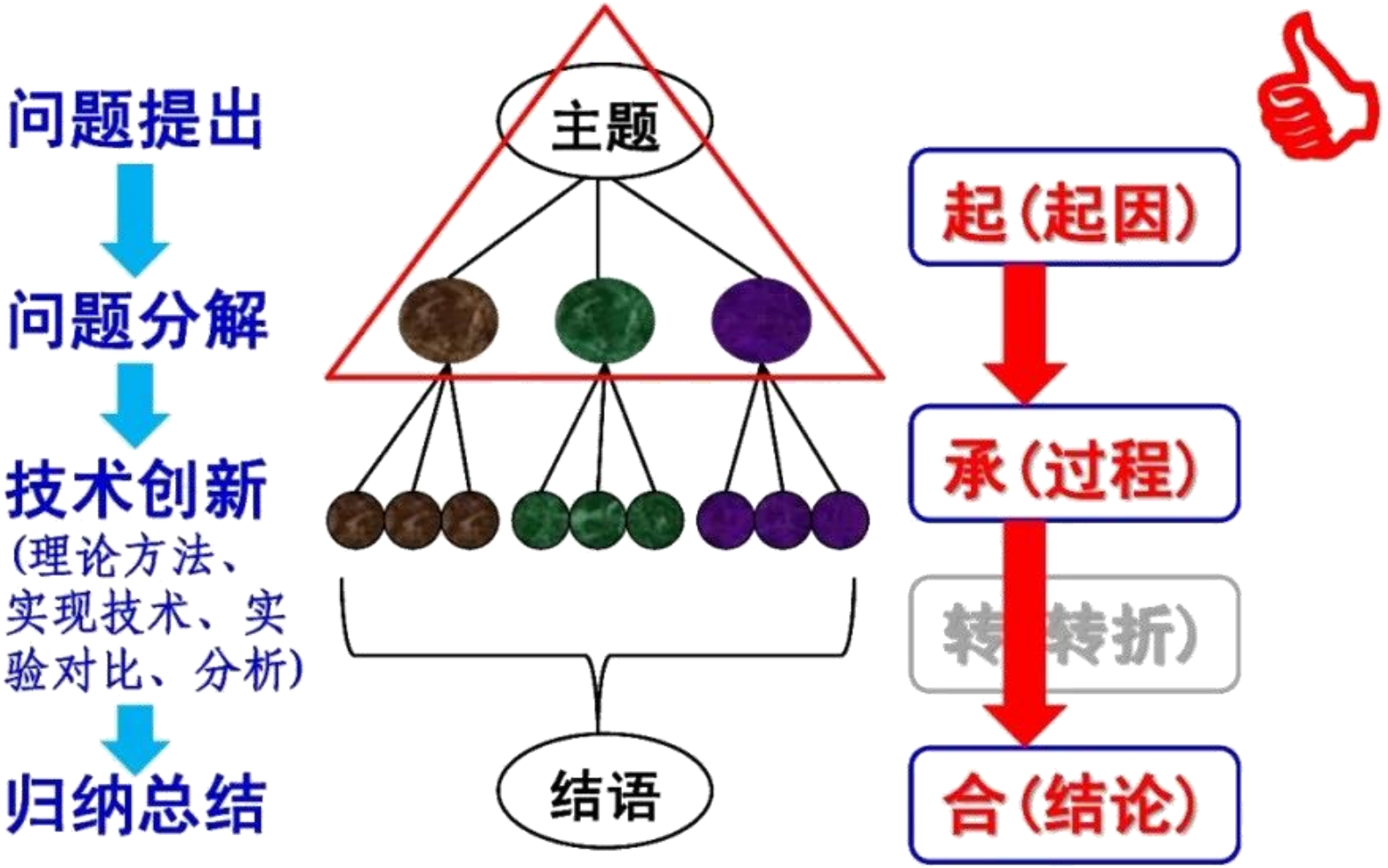

自顶向下(Top-Down)瀑布式的展开方式

整体布局

- 阐述方式

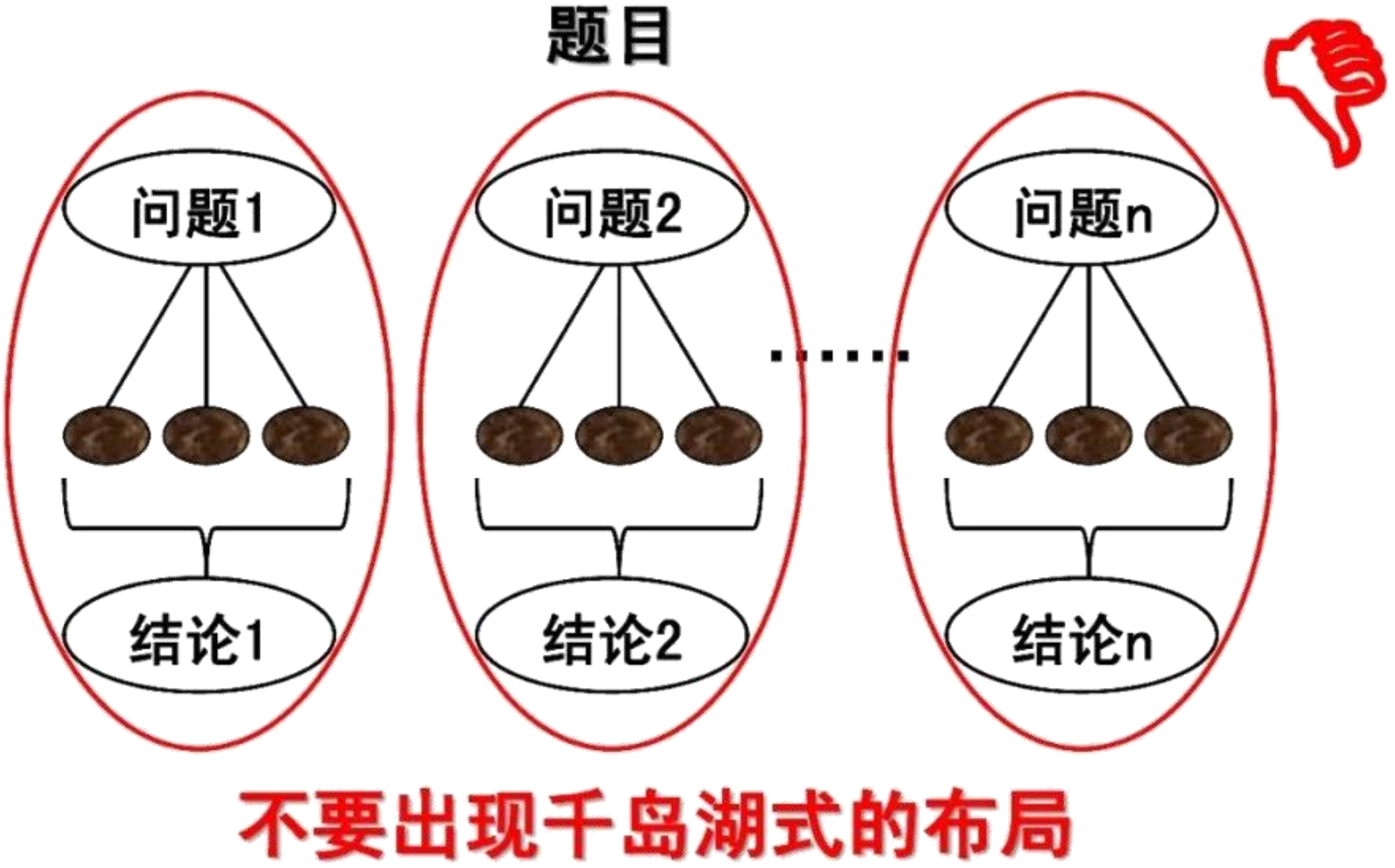

整体布局

- 内容分配

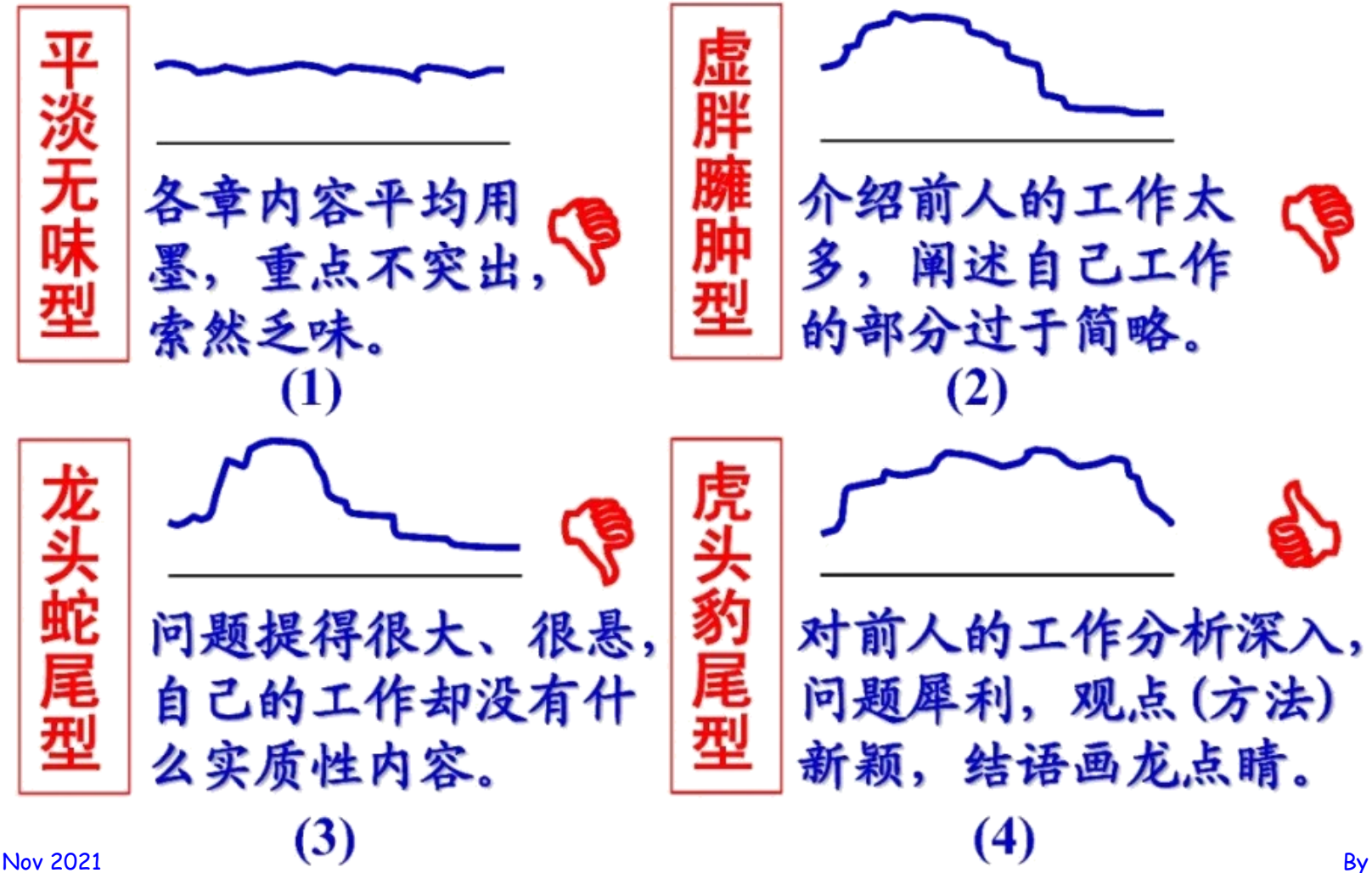
平淡无味型
各章内容平均用墨，重点不突出，索然乏味。
(1)
虚胖臃肿型
介绍前人的工作太多，阐述自己工作的部分过于简略。
(2)
龙头蛇尾型
问题提得很大、很悬，自己的工作却没有什么实质性内容。
(3)
虎头豹尾型
对前人的工作分析深入，问题犀利，观点(方法)新颖，结语画龙点睛。
(4)

整体布局

- 常见提纲
  - 第一章 绪论：简明扼要
    - 破题：基本概念和研究内容 （做什么？）
    - 意义：理论意义和应用价值 （为什么？）
    - 结构：主要贡献和结构安排 （怎么做？）

整体布局

- 常见提纲
  - 第二章 研究现状：深入浅出
    - 综述：针对拟研究的问题已有哪些工作和方法？
    - 分析：已有方法的优缺点对比，存在哪些缺陷？
    - 归纳：方法分类，问题归纳（预示本文的工作）
    - 动因：阐述自己的思路，进行问题分解
  - 切忌
    - 罗列已有的工作，面面俱到，没有自己的观点
    - 追溯历史太久远，涵盖范围太宽泛
    - 照抄别人的文献
  - 注
    - 也可将本章与第一章合并

整体布局

- 常见提纲
  - 第三~五章 创新工作：理论与实验并重
    - 阐述自己最重要的创新点
    - 注意各个创新点之间的关联
    - 有充分的实验对比和结果分析
    - 给自己的方法起一个响亮的名字
  - 注
    - 创新点不宜太多，一般为三个

整体布局

- 常见提纲
  - 第六章 总结展望：画龙点睛
    - 归纳全文的创新点
    - 指出需要进一步开展的工作
  - 切忌
    - 重复前面的摘要或绪论
    - 对下一步工作的展望太虚、太大

常见问题

- 题目太大、太泛，没有特色
- 主题不聚焦，研究内容缺乏整体性，各章内容相互独立
- 综述前人工作时只是简单地罗列，缺乏深入的分析和归纳总结
- 大篇幅地引用他人的工作，引用的图、表、公式、数据等不标明来源出处
- 贡献不明确，创新点不突出
- 实验对比的方法或系统不是本领域公认的
- 实验对比不充分，缺乏深入分析

注重细节

- 文字表达应通顺，含义明确，避免使用华丽地辞藻
  - 句子不通顺，含义模糊不清，例如：
    - **这些比较的都是应用在检索方面**，**是否**在分类任务中，其他的模型**是否**能发挥相应地优势还没……
  - 整段所表达的意思不明确
  - 出现半截句。例如：
    - 本论文提出如何利用条件随机场解决……问题
    - 本论文提出**了**如何利用条件随机场解决……问题**的方法**
  - 口语化严重，过多地使用“我们”
  - 用词过分华丽，尤其是在致谢中

注重细节

- 避免出现错别字，差错率不应超过1/10000
  - 常被忽视的错误：“的”与“地”不分
  - 不可容忍地错误：
    - 人名错误
    - 拼写错误：split → spit, from → form, window → widow
  - 不可忽视英文摘要
- 避免使用直接截图、粘贴的编辑方式，不要汉英混用
  - 直接从已发表的论文中截取图、表，粘贴到自己的论文中
  - 图、表及标题中使用英文，且无任何汉语注释

注重细节

- 字体、字号应统一，格式应规范
  - 章、节标题，正文格式符合给定模板
  - 公式中的变量字母大/小写、正/斜体要一致（公式内一致且与正文一致）
- 图、表、公式的编号格式应统一，且与正文中的引用一致
  - 采用每章独立计数方式，例如：
    - 图1-1，表2-2，公式（3-3）等
- 术语使用要规范、统一
  - 使用正确的术语，英文缩写首次出现时应给出全拼，对应缩写的英文字母应与缩写的大/小写保持一致，例如：
    - 从运动恢复结构 (Structure from Motion, SfM)
    - 同时定位与构图 (Simultaneous Localization And Mapping, SLAM)

注重细节

- 可以给自己的方法起个响亮、好记得名字，适当地拔高，但切勿口出狂言
  - 名字的英文字母不宜太长，一般不超过五个字母
  - 尽量不要使用“提出了……理论体系”，“解决了……问题”，“首次提出了……”等类似得表述
- 参考文献信息应详细，**格式统一**，正文中得引用应在参考文献中找到唯一的对应，切勿遗漏。尽量引用本领域内国际上公认的有代表性的重要之作，尤其是近几年的
  - 参考文献的排列顺序以及具体格式要严格按照给定模板

结束语

- 评价一篇论文优劣**最重要的标准**是看其解决的问题是否重要，创新点是否突出，实验是否充分可靠
- 论文的结构是否清晰，逻辑是否清楚，表达是否流畅、准确，具有非常重要的意义
- 我们提倡规范、严谨、朴实的写作风格，“标新立异”应体现在创新思想上，而不是体现在写作形式上
- 应遵循不同学科领域的论著写作规范

参考资料

- 宗成庆：如何撰写毕业论文

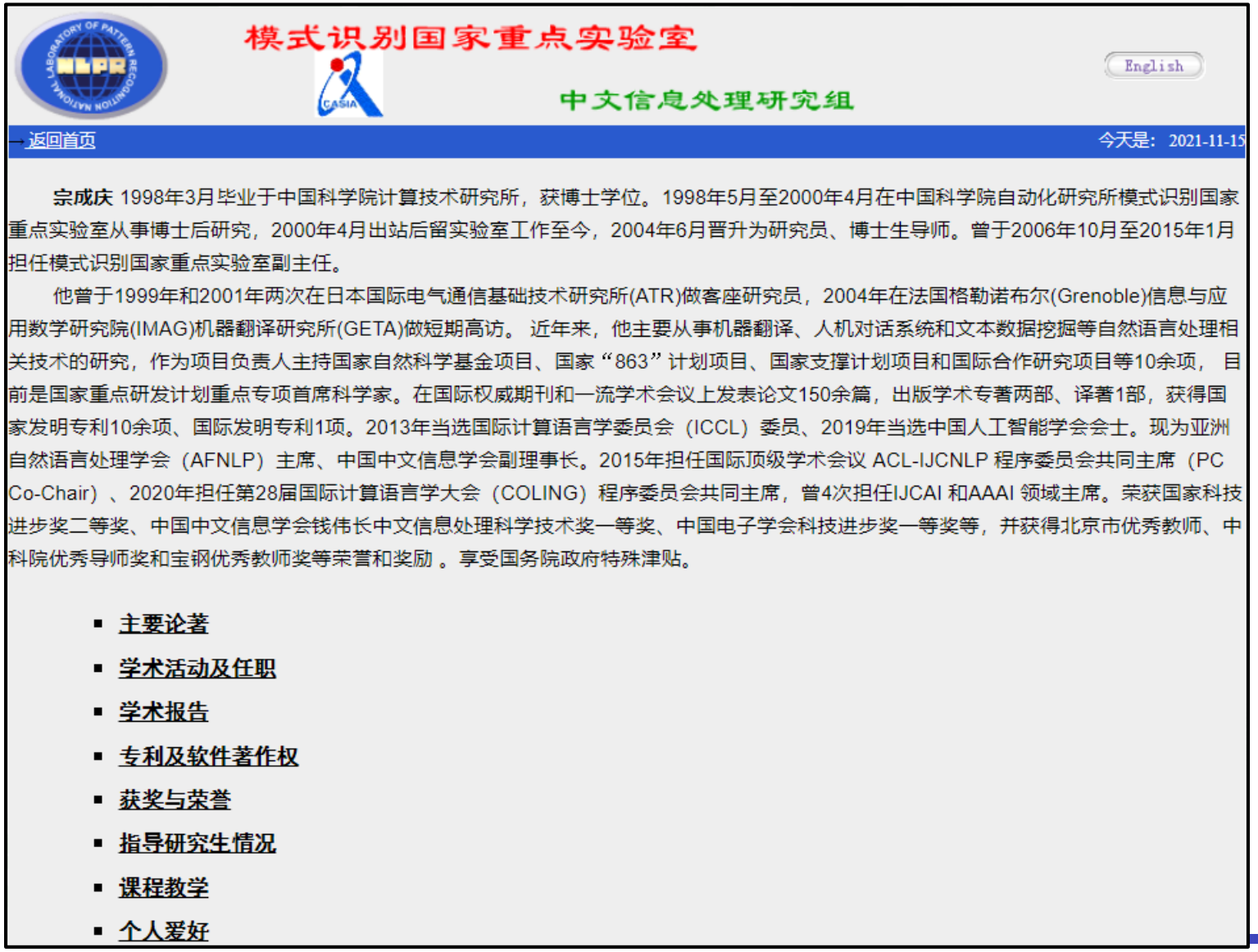

模式识别国家重点实验室

中文信息处理研究组

English

返回首页　　今天是：2021-11-15

宗成庆 1998年3月毕业于中国科学院计算技术研究所，获博士学位。1998年5月至2000年4月在中国科学院自动化研究所模式识别国家重点实验室从事博士后研究，2000年4月出站后留实验室工作至今，2004年6月晋升为研究员、博士生导师。曾于2006年10月至2015年1月担任模式识别国家重点实验室副主任。

他曾于1999年和2001年两次在日本国际电气通信基础技术研究所(ATR)做客座研究员，2004年在法国格勒诺布尔(Grenoble)信息与应用数学研究院(IMAG)机器翻译研究所(GETA)做短期高访。 近年来，他主要从事机器翻译、人机对话系统和文本数据挖掘等自然语言处理相关技术的研究，作为项目负责人主持国家自然科学基金项目、国家“863”计划项目、国家支撑计划项目和国际合作研究项目等10余项， 目前是国家重点研发计划重点专项首席科学家。在国际权威期刊和一流学术会议上发表论文150余篇，出版学术专著两部、译著1部，获得国家发明专利10余项、国际发明专利1项。2013年当选国际计算语言学委员会（ICCL）委员、2019年当选中国人工智能学会会士。现为亚洲自然语言处理学会（AFNLP）主席、中国中文信息学会副理事长。2015年担任国际顶级学术会议 ACL-IJCNLP 程序委员会共同主席（PC Co-Chair）、2020年担任第28届国际计算语言学大会（COLING）程序委员会共同主席，曾4次担任IJCAI 和AAAI 领域主席。荣获国家科技进步奖二等奖、中国中文信息学会钱伟长中文信息处理科学技术奖一等奖、中国电子学会科技进步奖一等奖等，并获得北京市优秀教师、中科院优秀导师奖和宝钢优秀教师奖等荣誉和奖励 。享受国务院政府特殊津贴。

- 主要论著
- 学术活动及任职
- 学术报告
- 专利及软件著作权
- 获奖与荣誉
- 指导研究生情况
- 课程教学
- 个人爱好

Practice Makes Perfect

Xiang Gao, Lecturer

E-mail: xgao@ouc.edu.cn | Web: https://ouc-xgao.github.io/

College of Engineering, Ocean University of China